FEDERAL UNIVERSITY OF UBERLANDIA
FACULTY OF ELECTRICAL ENGINEERING

Identification and characterization of short-term motor patterns in rest tremor of individuals with Parkinson's disease

Amanda Gomes Rabelo

Uberlândia/MG – 2023

AMANDA GOMES RABELO

Identification and characterization of short-term motor patterns in rest tremor of individuals with Parkinson's disease

Tese de Doutorado apresentada ao Programa de Pós-Graduação em Engenharia Elétrica da Universidade Federal de Uberlândia, como requisito parcial para Obtenção do título de Doutor em Ciências.

Orientador: Prof. Dr. Adriano de Oliveira Andrade (UFU)

Coorientador: Prof. Dr. Rodrigo Maximiano Antunes de Almeida (UNIFEI)

Uberlândia/MG - 2023

Ficha Catalográfica Online do Sistema de Bibliotecas da UFU
com dados informados pelo(a) próprio(a) autor(a).

R114 Rabelo, Amanda Gomes, 1989-
2023 Identification and characterization of short-term motor patterns in rest tremor of individuals with Parkinson's disease [recurso eletrônico] / Amanda Gomes Rabelo. - 2023.

Orientador: Adriano de Oliveira Andrade.
Coorientador: Rodrigo Maximiano Antunes de Almeida.
Tese (Doutorado) - Universidade Federal de Uberlândia, Pós-graduação em Engenharia Elétrica.
Modo de acesso: Internet.
Disponível em: http://doi.org/10.14393/ufu.te.2023.515
Inclui bibliografia.
Inclui ilustrações.

1. Engenharia elétrica. I. Andrade, Adriano de Oliveira,1975-, (Orient.). II. Almeida, Rodrigo Maximiano Antunes de,1984-, (Coorient.). III. Universidade Federal de Uberlândia. Pós-graduação em Engenharia Elétrica. IV. Título.

CDU: 621.3

Bibliotecários responsáveis pela estrutura de acordo com o AACR2:
Gizele Cristine Nunes do Couto - CRB6/2091
Nelson Marcos Ferreira - CRB6/3074

AMANDA GOMES RABELO

Identification and characterization of short-term motor patterns in rest tremor of individuals with Parkinson's disease

Tese de Doutorado apresentada ao Programa de Pós-Graduação em Engenharia Elétrica da Universidade Federal de Uberlândia, como requisito parcial para Obtenção do título de Doutor em Ciências.

Membros da banca:

Prof. Dr. Adriano de Oliveira Andrade, Orientador (UFU)

Prof. Dr. João Paulo Folador, Examinador (UFPR)

Prof. Dr. Thiago Ribeiro Teles dos Santos, Examinador (UFU)

Prof. Dr. Pedro Cunha Carneiro, Examinador (UFU)

Prof. Dr. Denis Delisle Rodriguez, Examinador (ISD)

Uberlândia/MG - 2023

UNIVERSIDADE FEDERAL DE UBERLÂNDIA
Coordenação do Programa de Pós-Graduação em Engenharia Elétrica
Av. João Naves de Ávila, 2121, Bloco 3N - Bairro Santa Mônica, Uberlândia-MG, CEP 38400-902
Telefone: (34) 3239-4707 - www.posgrad.feelt.ufu.br - copel@ufu.br

ATA DE DEFESA - PÓS-GRADUAÇÃO

Programa de Pós-Graduação em:	Engenharia Elétrica				
Defesa de:	Tese de Doutorado, 324, PPGEELT				
Data:	Trinta de agosto de dois mil e vinte e três	Hora de início:	08:00	Hora de encerramento:	10:44
Matrícula do Discente:	11713EEL002				
Nome do Discente:	Amanda Gomes Rabelo				
Título do Trabalho:	Identification and characterization of short-term motor patterns in rest tremor of individuals with Parkinson's disease				
Área de concentração:	Processamento da Informação				
Linha de pesquisa:	Processamento Digital de Sinais e Redes de Computadores				
Projeto de Pesquisa de vinculação:	Coordenador do projeto: Adriano de Oliveira Andrade Título do projeto: AVALIAÇÃO OBJETIVA E LONGITUDINAL DE SINAIS CARDINAIS DA DOENÇA DE PARKINSON Agência financiadora: CNPQ Número do processo na agência financiadora: 304818/2018-6 Vigência do projeto: 2019 - 2023				

Reuniu-se por meio de videoconferência, a Banca Examinadora, designada pelo Colegiado do Programa de Pós-graduação em Engenharia Elétrica, assim composta: Professores Doutores: Thiago Ribeiro Teles dos Santos - FAEFI/UFU; Pedro Cunha Carneiro - FEELT/UFU; João Paulo Folador - UFPR; Denis Delisle Rodriguez - ISD e Adriano de Oliveira Andrade - FEELT/UFU, orientador(a) do(a) candidato(a).

Iniciando os trabalhos o(a) presidente da mesa, Dr. Adriano de Oliveira Andrade, apresentou a Comissão Examinadora e a candidata, agradeceu a presença do público, e concedeu a Discente a palavra para a exposição do seu trabalho. A duração da apresentação da Discente e o tempo de arguição e resposta foram conforme as normas do Programa.

A seguir o senhor presidente concedeu a palavra, pela ordem sucessivamente, aos examinadores, que passaram a arguir a candidata. Ultimada a arguição, que se desenvolveu dentro dos termos regimentais, a Banca, em sessão secreta, atribuiu o resultado final, considerando a candidata:

Aprovada.

Esta defesa faz parte dos requisitos necessários à obtenção do título de Doutor.

O competente diploma será expedido após cumprimento dos demais requisitos, conforme as normas do Programa, a legislação pertinente e a regulamentação interna da UFU.

Nada mais havendo a tratar foram encerrados os trabalhos. Foi lavrada a presente ata que após lida e achada conforme, foi assinada pela Banca Examinadora.

Documento assinado eletronicamente por **Adriano de Oliveira Andrade**, **Professor(a) do Magistério Superior**, em 30/08/2023, às 10:49, conforme horário oficial de Brasília, com fundamento no art. 6º, § 1º, do Decreto nº 8.539, de 8 de outubro de 2015.

Documento assinado eletronicamente por **Pedro Cunha Carneiro**, **Professor(a) Substituto(a) do Magistério Superior**, em 30/08/2023, às 10:52, conforme horário oficial de Brasília, com fundamento no art. 6º, § 1º, do Decreto nº 8.539, de 8 de outubro de 2015.

Documento assinado eletronicamente por **João Paulo Folador**, **Usuário Externo**, em 30/08/2023, às 10:52, conforme horário oficial de Brasília, com fundamento no art. 6º, § 1º, do Decreto nº 8.539, de 8 de outubro de 2015.

Documento assinado eletronicamente por **Thiago Ribeiro Teles dos Santos**, **Professor(a) do Magistério Superior**, em 05/09/2023, às 09:51, conforme horário oficial de Brasília, com fundamento no art. 6º, § 1º, do Decreto nº 8.539, de 8 de outubro de 2015.

Documento assinado eletronicamente por **Denis Delisle Rodriguez**, **Usuário Externo**, em 14/09/2023, às 15:40, conforme horário oficial de Brasília, com fundamento no art. 6º, § 1º, do Decreto nº 8.539, de 8 de outubro de 2015.

A autenticidade deste documento pode ser conferida no site https://www.sei.ufu.br/sei/controlador_externo.php?acao=documento_conferir&id_orgao_acesso_externo=0, informando o código verificador **4673420** e o código CRC **24C8DCA1**.

Referência: Processo nº 23117.052403/2023-27 SEI nº 4673420

To Carlos Rabelo Veloso, Letícia Veloso Barros,

and Maria Flor Barros for inspiration.

You are symbols of resilience and love in my life.

Acknowledgments

Firstly, I would like to highlight the importance of pursuing a Ph.D., the Doctor of Philosophy. This degree represents the culmination of years of dedication, perseverance, and intellectual curiosity. It has provided me with the opportunity to delve into the depths of knowledge, explore new frontiers, and contribute to the ever-growing body of research. The pursuit of a Ph.D. has not only expanded my academic horizons but also honed my critical thinking, analytical skills, and ability to tackle complex problems.

I would like to express my heartfelt gratitude to the numerous individuals who have contributed to the completion of this thesis. Their support, guidance, and encouragement have played an invaluable role in my academic journey.

First and foremost, I am deeply indebted to my esteemed supervisors, Prof. Dr. Adriano Andrade and Prof. Dr. Rodrigo Antunes whose expertise and mentorship have been instrumental in shaping my research and academic growth. Their dedication, insightful feedback, and guidance have challenged me to push my boundaries and strive for excellence. I am truly grateful for their unwavering commitment to my development as a researcher.

I sincerely appreciate all the professors from UFU who have imparted their knowledge and expertise, laying the foundation for my academic pursuits. Especially, Prof. Dr. Luciane Sande, Prof. Dr. Marcus Fraga, and Prof. Dr Adriano Alves, have been with me since the beginning of my journey.

I would like to thank all my colleagues at the laboratories of NIATS and NTA, especially Viviane Lima, Ariana Moura, and João Paulo Folador. Their collaboration, support, and insightful discussions have enriched my research and provided a stimulating environment for academic exploration. Thank you to the professionals and patients from Associação de Parkinson do Triângulo Mineiro for the collaboration and support in all the research. The collective efforts of the research community have significantly contributed to the success of this thesis.

Thank you, Dr. Carolina Carneiro, for believing in me and pushing me beyond my limits. Your expertise, wisdom, and dedication have significantly impacted my personal and professional growth. I am truly fortunate to have had you as my mentor, and I will always cherish the lessons I've learned under your guidance. You showed me the true meaning behind this academic pursuit and opened my eyes to new career paths and possibilities.

I want to express my heartfelt appreciation to my remarkable team at Hospital Israelita Albert Einstein: Dr. Adriano Pereira, Dr. Uri Flato, Dr. Cesar Truyts, Daniel Lages, Andreia Pardini, and Mariana Pires. Your support and collaboration have played an instrumental role in shaping me

into the fulfilled and accomplished professional I am today. I am grateful for the joy and sense of fulfillment you have brought into my life, transcending borders and making a profound impact.

To my dear family and friends, I am forever grateful for your unwavering love, encouragement, and understanding throughout this academic journey. Your presence, support, and belief in me have been a constant source of strength and motivation.

Abstract

Tremor serves as a significant biomarker for various diseases, including Parkinson's Disease, and plays a crucial role in monitoring disease progression, assessing treatment efficacy, and aiding in the diagnosis of movement disorders. Despite considerable progress in tremor research over the past thirty-eight years, challenges still remain in understanding the nature of tremors and within-individual fluctuations. A deeper understanding of tremors can lead to personalized treatment approaches and optimize pharmacogenomics studies for the pathology. The objective of this research is to identify and characterize the Short-Term Motor Patterns (STMPs) present in the rest tremor signal using inertial sensors. STMPs manifest in the signal in less than 1 second and exhibit self-similar structures across multiple time scales. They have a hidden dynamic with underlying structures contributing to the abnormal movement observed in tremors. The study involved healthy individuals (N = 12, mean age 60.1 ± 5.9 years) and individuals with Parkinson's Disease (N = 14, mean age 65 ± 11.54 years). Signals were collected using a triaxial gyroscope placed on the dorsal side of the hand during a resting condition. The data were pre-processed, and seven features were extracted from each 1-second window with 50% overlap. The STMPs were identified using the k-means clustering technique applied to the data in the two-dimensional space generated by t-Distributed Stochastic Neighbor Embedding (t-SNE). The frequency, transition probability, and duration of the STMPs were assessed for each group. All STMP features were averaged across the groups. Three distinct STMPs (STMP1, STMP2, and STMP3) were identified in the tremor signals ($p < 0.05$). STMP1 was predominant in the healthy control (HC) subjects, STMP2 was present in both the healthy and Parkinson's disease group, and STMP3 was observed in the Parkinson's disease group. Only the coefficient of variation and complexity not showed significant differences between the groups. Regarding signal dynamics, signals from individuals with Parkinson's disease tended to exhibit lower STMP transition probabilities and longer durations of STMP than the healthy control subjects. These findings can assist professionals in characterizing and evaluating the severity of tremors and assessing treatment efficacy.

Keywords:

Empirical Mode Decomposition; k-means; gyroscope; Parkinson’s disease; rest tremor; short-term motor patterns (STMPs); t-SNE

Resumo

O tremor é um significante biomarcador para várias doenças, incluindo a doença de Parkinson e desempenha um papel fundamental no monitoramento da progressão da doença, na avaliação da eficácia de tratamentos e auxiliando no diagnóstico. Apesar do considerável progresso das pesquisas envolvendo tremor nos últimos 30 anos, ainda existem desafios na compreensão da natureza do tremor e nas flutuações individuais. Uma compreensão profunda dos tremores pode auxiliar em tratamentos personalizados e otimizar estudos de fármacos para a patologia. O objetivo dessa pesquisa é identificar e caracterizar os padrões motores de curto prazo (STMPs) presentes no sinal do tremor por meio do giroscópio. Os STMPs manifestam no sinal em uma janela menor que 1 segundo e exibem estruturas auto-semelhantes em múltiplas escalas de tempo. Eles possuem uma dinâmica oculta com estruturas subjacentes que contribuem para o movimento anormal observado nos tremores. Este estudo envolveu indivíduos hígidos, no grupo controle (N = 12, media idade 60.1 ± 5.9 anos) e indivíduos com a doença de Parkinson (N = 14, media idade 65 ± 11.54 anos). Os sinais foram coletados usando um giroscópio triaxial posicionado no dorso da mão dominate durante a coleta em repouso. Os dados foram pré-processados e sete características foram extraídas de cada janela de 1 segundo com 50% de sobreposição. Os STMPs foram identificados usando a técnica de clusterização k-menas aplicada ao espaço bidimensional gerados pelo t-Distributed Stochastic Neighbor Embedding (t-SNE). A frequência, probabilidade de transição e tempo de duração dos STMPs foram avaliados para cada grupo. Todas as medias das caracteríticas extraídas dos STMPs foram calculados entre os grupos. Três STMPS distintos (STMP1, STMP2, and STMP3) foram identificados no sinal do tremor ($p<0.05$). O STMP1 foi predominante em indivíduos do grupo controle, o STMP2 estava presente em ambos os grupos, e o STMP3 foi mais recorrente no grupo co com a doença de Parkinson. Somente o coeficiente de probabilidade e complexidade não apresentaram diferença significativa entre os grupos. Com relação a dinâmica dos sinais, sinais de indivíduos com a doença de Parkinson tendem a possuir a probabilidade de transição entre STMPs menor e maior tempo de duração no STMP quando comparado ao grupo controle. Esses achados podem auxiliar profissionais na caracterização e avaliação da severidade do tremor e avaliação da eficácia de tratamentos.

Palavras-chave:

Empirical Mode Decomposition; k-means; giroscópio; doença de Parkinson; tremor de repouso; padrões motores de curto prazo (STMP); t-SNE

List of Figures

List of Tables

Abbreviations

STMPs - Short-Term Motor Patterns

PD - Parkinson's disease

NINDS - National Institute of Neurological Disorders and Stroke

MDS-UPDRS - Movement Disorder Society United Parkinson's Disease Rating Scale

MAO-B - Monoamine Oxidase-B

RT - Rest Tremor

EMD - Empirical Mode Decomposition

IMF - Intrinsic Mode Functions

LPFs - Local Field Potentials

ML - Machine Learning

STN - Subthalamic Nucleus

HFO - High-Frequency Oscillations

MDS - Movement Disorder Society

EDA - Exploratory Data Analysis

HG - Healthy Group

HC - Healthy Control

IMUs - Inertial Measurement Units

TRMS - Tukey’s Running Median Smoothing

PSD - Power Spectral Density

FT - Fourier Transform

MAV - Mean Absolute Value

CV - Coefficient of Variation

ZCR - Zero Crossing Rate (ZCR)

SampEn - Sample Entropy

ACT - Activity

MOB - Mobility

COMP - Complexity

EEG - Electroencephalogram

FFT - Fast Fourier Transform

t-SNE - t-Stochastic Neighborhood Embedding

KL - Kullback Leibler

Contents

1. Introduction

1.2 Problem Formulation

This thesis aims to address the problem of identifying and characterizing short-term motor patterns (STMPs) present in the structure of rest tremors using inertial sensors. Unlike other cardinal signals in Parkinson's disease (PD) that have been well characterized, tremors remain poorly understood due to the involvement of different mechanisms mediating the various tremor types observed in clinical neurology [1]. Given this inherent heterogeneity, a tremor is considered a complex signal.

The main issue is that most tremor studies overlook this complexity and solely focus on detecting and distinguishing different types of tremors [2]–[5]. However, exploring the short-term patterns of the tremor signal has the potential to provide new insights into the origin and underlying mechanisms of this symptom. Additionally, gaining a better understanding of tremors can lead to individualized treatment approaches and optimizing pharmacogenomics studies for the pathology [6], [7].

To address this problem, an experimental protocol was developed to identify and characterize, systematically, STMPs in rest tremors of healthy individuals and those with Parkinson's disease.

1.2 Relevance of the Thesis

Tremor is a significant biomarker for various diseases, playing a crucial role in disease progression monitoring, treatment efficacy assessment, and supporting the diagnosis of movement disorders. Despite significant advancements in tremor research over the past thirty-eight years, as highlighted in the comprehensive review by Leslie J. Findley and Rudy Capildeo, there are still remaining challenges in the field [8].

One such challenge is identifying and characterizing STMPs in tremors using inertial sensors. These STMPs have the potential to provide valuable insights into the underlying mechanisms responsible for tremors, and they can be observed in both healthy individuals and those with Parkinson's disease. Gaining a better understanding of STMPs can lead to the development of improved therapies and enhance the monitoring of different types of pathological tremors.

By addressing the research gap related to STMPs in tremors using inertial sensors, this thesis aims to contribute to the field by advancing our knowledge of tremor characteristics and mechanisms. Ultimately, this research can potentially improve treatment strategies and enhance the management of tremor-related conditions.

1.3 The Main Aim of the Research

The objective of this thesis is twofold: (i) to identify the presence of short-term motor patterns in resting tremors exhibited by individuals with Parkinson's disease as well as physiological tremors, and (ii) to characterize these STMPs in terms of their amplitude, persistence, and regularity.

1.4 The Objectives of the Thesis

To address the stated problem and achieve the objectives of the thesis, the following tasks were formulated:

- Conduct an investigation into the most effective strategies for pre-processing tremor signals using exploratory data analysis.
- Explore and select relevant features for the proposed analysis.
- Investigate machine learning tools that facilitate the selection of appropriate amounts of STMPs.
- Explore tools for characterizing STMPs.
- Investigate various visualization techniques to effectively communicate the findings of the study.

1.5 Scientific Novelty of the Thesis

- The analysis reveals the existence of at least three distinct types of STMPs in physiological and Parkinson’s disease.
- The type and severity of the tremor influence the presence of STMPs in the signal. Individuals with Parkinson's disease exhibit lower transition values and longer duration of STMPs compared to healthy individuals.

1.6 Practical Value of the Research Findings

The findings of this research have practical implications in the field of tremor analysis. The results can be used for monitoring and characterizing tremors, including psychological tremors, which can assist professionals in evaluating the stage of tremor and the effectiveness of treatments. Additionally, these findings have the potential to contribute to personalized medicine and early diagnosis of tremors.

1.7 Structure of the thesis

The thesis consists of an introduction, eight chapters, and general conclusions. The volume of the thesis is 79 pages, in which are given: 26 figures and 8 tables. Additionally, in the thesis 104 items are cited.

2. Literature Survey of Parkinson's Disease

James Parkinson first described Parkinson's disease as "shaking palsy" in 1817. Currently, the clinical manifestations of PD include tremor, rigidity, bradykinesia (slowness of movement), and postural instability as the cardinal motor symptoms [9].

PD is the second most common motor condition, with about 6.1 million people affected worldwide in 2016 [10]. The incidence and prevalence of this disease have risen in the past 20 years. The personal impact is enormous. Its progression affects patients, families, and caregivers. Also, PD impacts society by accumulating a mounting socioeconomic burden [10].

2.1 Pathophysiology

The hallmark pathology of PD is the degeneration of dopaminergic neurons in the substantia nigra compacta, accompanied by the development of abnormal intracellular aggregates called Lewy Bodies (Figure 1).

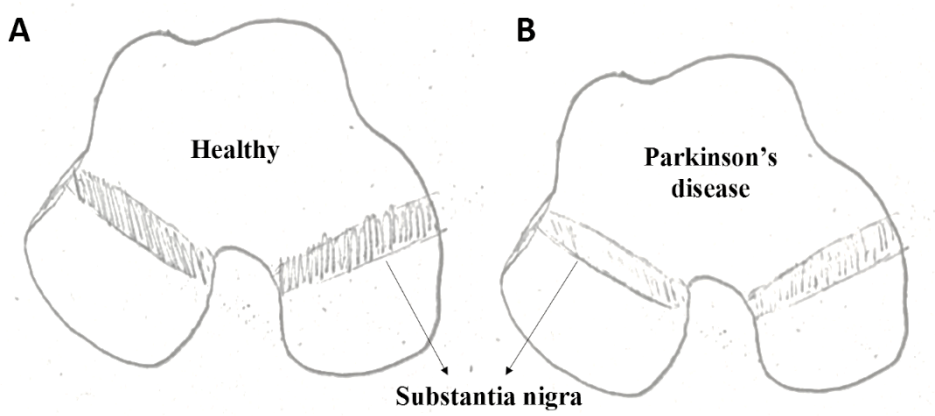

Figure 1: In a brain of a person with Parkinson's disease, the substantia nigra is well defined (Figure 1-A), but in a brain affected by Parkinson's disease the substantia nigra appears visibly diminished (Figure 1-B).

The accumulation of Lewy bodies blocks dopamine's production and transmission, resulting in movement issues of PD, which can begin years or even decades before visible symptoms manifest, causing severe motor control impairment [9].

Despite the significant progress made in understanding the pathological and biochemical changes associated with the disease, since the initial description by Ehringer and Hornykiewicz in 1960 [11], the underlying degenerative process affecting the substantia nigra pars compacta remains unknown. No single causative factor has been identified. Recent research suggests that a combination of factors, including environmental stress, drug exposure, low-level inflammation, aging, mitochondrial defects, oxidative stress, glutamate toxicity, and genetic factors, may contribute to the etiopathogenesis of PD. This suggests that PD is likely to have a multifactorial etiology [9].

PD manifests itself through various motor symptoms and signals, suggestting that it may not be a singular condition but rather a complex combination of multiple diseases [12]–[14]. This conclusion is based on the observed heterogeneity of the disease among patients, as well as the absence of a single biomarker or treatment for the development or progression of Parkinson's [13]. Because of that, several studies explore predictive models to elucidate the underlying mechanisms of dopaminergic denervation in the substantia nigra compacta in PD [9].

The tremor experienced by individuals with PD cannot be simply attributed to a lack of dopamine in the basal ganglia, as other neurotransmitter systems and brain regions are also implicated. Additionally, tremors advance at their own rate and the severity of tremors does not necessarily correspond with the severity of bradykinesia and rigidity [1].

2.2 Clinical Presentation

Parkinson's disease manifests as a complex interplay of four main components: motor symptoms, and cognitive changes, behavioral/neuropsychiatric changes, and autonomic nervous system dysfunction denoted as non-motor symptoms. The prominence of these components may vary among individuals, leading to unique clinical presentations.

Motor symptoms:

- Tremor
- Bradykynesia
- Rigidity
- Postural Instability

Non-motor symptoms:

- Problems with decision-making, multi-tasking, memory retrieval, and visuospatial
- Urinary Urge/Incontinence
- Constipation
- Gastropatresis
- Olfactory dysfunction (Anosmia)
- Insomnia
- Dementia
- Depression

2.3 Diagnosis

Diagnosing PD relies on clinical criteria, as there is no definitive test for diagnosis. In the past, confirmation of the hallmark Lewy body on autopsy was considered the gold standard for diagnosis [15]. In clinical practice, PD is typically diagnosed based on a combination of cardinal

motor features, associated and exclusionary symptoms, and response to levodopa. However, differentiating PD from other forms of parkinsonism can be challenging, especially in the early stages of the disease when signs and symptoms may overlap with other syndromes [16], [17].

To aid in diagnosis, specific diagnostic criteria have been developed by organizations such as the UK Parkinson's Disease Society Brain Bank and the National Institute of Neurological Disorders and Stroke (NINDS), which provide guidelines for clinicians to assess the presence of PD based on a standardized set of clinical features and findings [18]. Additionally, neuroimaging, drug tests, and scales, such as the Movement Disorder Society United Parkinson's Disease Rating Scale (MDS-UPDRS), may also be used to support the diagnostic process. The MDS-UPDRS is a primary clinical tool used to evaluate PD and is divided into four sections, with Part III dedicated to assessing motor symptoms, allowing for evaluation of motor signs in different body regions [19].

2.4 Therapies

Although Parkinson's disease currently lacks a cure, adopting healthy habits such as maintaining a balanced diet, engaging in regular exercise, psychological and physiotherapy treatment, utilizing certain medications, and surgical therapies can potentially mitigate the impact of its signs and symptoms [20]. As previously stated, PD presents itself in a unique manner for each individual, necessitating a personalized approach to treatment. The appropriate therapeutic strategies will depend on various factors including the patient's age, stage of the disease, troublesome symptoms, and the potential benefits and risks associated with specific treatments [21].

The treatment of PD using pharmacological approaches focuses on addressing the deficit of dopamine or inappropriate imbalances of dopamine and other neurotransmitters. According to the American Academy of Neurology, drug therapy should be started once patients begin to exhibit functional disability [22]. There are many types of drugs employed in the treatment of motor symptoms in individuals with PD, such as Carbidopa/levodopa (Sinemet), both ergot and non-ergot types of dopamine agonists, monoamine oxidase-B (MAO-B) inhibitors, injectable dopamine agonist (apomorphine, or Apokyn), N-methyl-DAspartate receptor inhibitors, and anti-cholinergics. Levodopa, non-ergot dopamine agonists such as pramipexole (Mirapex) and ropinirole (Requip), and MAO-B inhibitors such as selegine (Eldepryl) and rasagiline (Azilect) [20].

While these medications are effective in addressing certain motor symptoms such as bradykinesia, research has demonstrated that they are less effective in treating tremors [23]. The response of resting tremor, for instance, in individuals with PD to dopaminergic treatment varies compared to other motor symptoms such as rigidity and bradykinesia [24]. Although

dopaminergic drugs can reduce tremors, there is no medication that consistently alleviates resting tremor in PD [23], [24]. A significant percentage of individuals with PD do not experience a reduction in tremors despite taking levodopa and dopaminergic medications. This variable response has led to a novel classification of tremors based on their responsiveness to dopamine treatment, including dopamine-responsive and dopamine-resistant subtypes [25].

3. Literature Survey on Tremor

3.1 Landmarks in tremor research

Tremor is a rhythmical and involuntary oscillatory movement of a body part that can be a physiological tremor, manifested in healthy individuals, or a pathological tremor, a symptom in individuals who suffer from any disorder [26]. Because of that, it has been widely investigated. Horsley and Schafer (1886) were the first authors to measure the tremor characterizing it by overlapped 10-Hz tremulous twitches [27]. Then, investigations about the basis of neurogenic tremors came out (Figure 2).

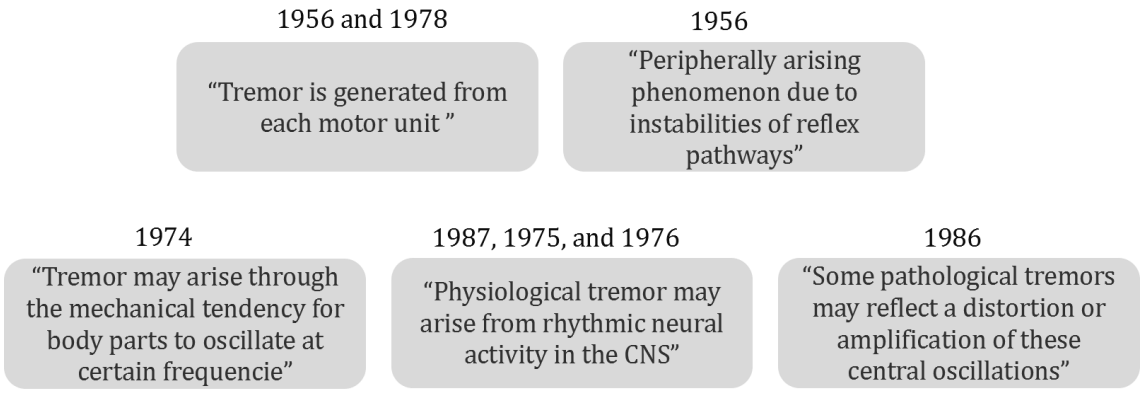

Figure 2: Review of the neurogenic mechanism of tremor generation according to [26].

From these investigations, other hypotheses arose that the central oscillations may be linked to the tremors. Moreover, they concluded that psychological tremor, for instance, is the summation of some oscillations across a frequency range represented in the EEG, not a pure 10-Hz range oscillation [26].

From these hypotheses, they concluded that a clear comprehension of the tremor origin would mean understanding better the rhythmic nature of human motor control [26]. However, even after 70 years of research, the tremor's origin remains unclear and has been investigated in many studies [4], [6], [7], [28]. For instance, the physiological tremor origin is unlikely to be caused by neurogenic distortion. On the other hand, in PD, there is no consensus about its origin [26]. Some studies have linked the cause of tremors to the oscillating activity of the thalamus, while others have linked it to the basal ganglia [29]. As claimed a priori, understanding the tremor's basis plays a crucial role in tremor evaluation and the improvement of therapies for different types of pathological tremors. Because of that, the following sections will provide an overview of the physiological tremor and Parkinson's tremor.

3.2 Types of tremors

As mentioned above, there are various types of tremors that can be classified as either physiological or pathophysiological [26].

When considered pathophysiological, they may be related to several diseases, such as Parkinson's disease, essential tremor, or Huntington's disease. Tremors can manifest differently depending on the affected limb position, such as rest tremor or kinetic tremor [1], [26].

In Parkinson's disease, tremors usually affect the upper limbs, but they may also manifest in other body areas. While rest tremors are more common in Parkinson's disease, individuals with Parkinson's disease may present with multiple subtypes of tremors, including postural, kinetic, and re-emergent (tremor that appears after a delay while the arms are maintained in an outstretched position) [1], [30].

In this study, we aim to explore rest tremors in PD and compare them to physiological tremors observed in a control group.

3.2.1 Physiological tremor

The physiological tremor has a smaller amplitude and is present in all subjects. It becomes more visible during muscular fatigue, anxiety, emotional stress, fear, excitement, or under-drug effects. Its frequency range is around 8-12 Hz in younger people and 6-7 Hz in older ones [31].

The uncertainty remains considerable regarding the central origin of physiological tremors. Its origin is related to the different peripheral and central processes that can generate such oscillations [26].

3.2.2 Rest tremor in Parkinson's disease

In contrast to physiological tremor, pathological tremor presents higher amplitude and it may be associated with a disorder such as Parkinson's disease (PD) [26].

The most prevalent tremor in PD is the resting tremor [24], [29], [32]. This tremor manifests when a voluntary muscle contraction is absent in a certain body segment [29], and the duration and amplitude of this sign can be taken to characterise the complexity and severity of the disease.

Tremor in PD may cause severe disability and significantly reduce the quality of life [24]. Approximately 75% of people with PD experience tremor at some point during the course of the disease [32]. Even those individuals who do not have tremor report that it would be the most discomforting and disturbing symptom of PD [33].

Usually, the tremor is dominant on one side of the body, starting distally in the arms of individuals with PD [34], and the upper extremity is often more affected than the lower extremity [35]. It is not the only type of rest tremors that occurs in the disorder, as other types of tremor can be observed during postural and kinetic activities [35].

Tremor is characterized according to its frequency, amplitude, topographic distribution, depending on the task and position of the limb. According to this, tremor can be classified as rest tremor, postural tremor, and kinetic tremor [34]. Rest tremor (RT) occurs in any part of the body in the absence of voluntary muscular activity. The frequency range of RT is usually between 3 to 8 Hz. RT may disappear with action, and it also may be reduced by holding one hand with another or crossing the legs. The RT amplitude may increase during mental stress [34]. Postural tremor occurs in body parts while maintaining a posture, such as holding a cup, and it is triggered by keeping the limb against gravity. Postural tremor is typically in the 4 to 12 Hz frequency range [34]. Kinect tremor appears during limb movement, often worsening when the limb is near the target. Tremulous movements are perpendicular to the main direction of the intended movement and tend to predominate over proximal musculature. The frequency range is 2 to 12 Hz [34].

These types of tremor may appear in isolation or in combination. Postural or kinetic tremor may occur together with rest tremor, but with different frequencies. The rest tremor can occur with a postural tremor but disappears during a kinetic task [2].

Moreover, tremulous movements can be associated with other disorders, such as Essential tremor and cerebellar diseases [34]. A new consensus criterion for classifying tremor disorders was published in 2018 [36]. The aim was to provide a more detailed approach to tremor diagnosis based on two aspects, such as detailing clinical parameters and the etiological classifications [37]. This new approach intends to reduce misdiagnoses among these disorders.

3.2.2.1 Assessment of tremor in Parkinson's Disease

Tremor assessment plays a fundamental role in evaluating the progression of PD, determining the efficacy and adjustment of drug therapies, and identifying the underlying diagnosis of the disease [34], [37]. Currently, the MDS-UPDRS is the primary clinical tool to evaluate PD. This scale is divided into four sections, with Part III dedicated to assessing motor symptoms.

The scale can evaluate the motor signs of distinct body regions. However, there are specific MDS-UPDRS items that are exclusive for the assessment of hand tremors. This is justified by the fact that the body's extremities, such as the hand and arm, often are correlated to the onset of tremor. Furthermore, hand tremors are controlled by multiple physiological components, including the basal ganglia, cerebellar circuits, and peripheral nerves that interact in various tempo-spatial scales, responsible for motor control.

The tremor is ranked according to the amplitude of hand tremors during some tasks. The other limbs are also evaluated from items 3.17 and 3.18. This research considers the following MDS-UPDRS items for the evaluation of hand tremor [19]:

- item 3.15 evaluates postural tremor. “The hands are rated separately. The rating is based on the highest amplitude seen. The patient is instructed to stretch the arms out in front of the body with palms down. The wrist should be straight, and the fingers comfortably separated so that they do not touch each other. This posture should be observed for 10 seconds.”
- item 3.16 evaluates Kinect tremor. “The hands are rated separately. The rating is based on the highest amplitude seen. The patient is instructed to stretch the arms out in front of the body with palms down. The patient is instructed to perform finger-to-nose movements slowly at least 3 times.”
- item 3.17 evaluates rest tremor. “The hands are rated separately. The rating is based on the highest amplitude seen. The patient is instructed to sit quietly in a chair with the hands placed on the arms of the chair and the feet comfortably supported on the floor for 10 seconds.”
- item 3.18 evaluates the constancy tremor. “The rating is focused on the constancy of rest tremor during other tasks in which different body parts are in resting.”

The MDS-UPDRS scores for these items range from 0 to 4, where 0 represents the non-visible tremor, and 4 is the most severe sign. However, the use of MDS-UPDRS requires time and examiner’s experience, and therefore, several quantitative approaches have been developed to support the tremor assessment [2], [3], [5]. These analyses use different approaches to detect tremors based on sensors [4], [38], [39].

3.2.2.2 Objective evaluation of tremor

There is an ever-growing number of scientific research efforts to increase understanding of the tremor's mechanisms and the future [1]; it may help in following up the progress of Parkinson's disease, as well as in the adjustment of drug and surgical-based treatments.

The main focus of studies about tremor assessment involves accurate detection of the activity tremulous [40]–[42]. For instance, Huo et al. used inertial sensors to quantify the severity of PD symptoms and to differentiate PD patients from healthy subjects. In order to detect tremors, the raw data from the two gyroscopes and accelerometers were filtered with a Butterworth bandpass filter (2 - 12 Hz). The means and standard deviations of processed rates-of-turn and accelerations were used as feature inputs for tremor classification. The classifier presented high accuracy for estimating the UPDRS scores of Kinect tremor (accuracy = 91.8%), and postural tremor (accuracy of 80.2%) [40].

De Lima et al. introduced the Empirical Mode Decomposition (EMD) to study tremors, and they used gyroscopes to detect rest and kinetic tremor. They identified the intrinsic mode functions (IMF) that represent tremulous and voluntary activity. The result was compared with

the method traditional in which the cutoff frequencies are set in a digital filter, reinforcing the high accuracy of this method [41].

In the same context, Lee et al. used EMD for analyzing nonlinear and nonstationary primary bowing tremor in violinists and compared the results to the Fast Fourier transform method. The results showed that the IMF might represent the tremor and voluntary movement. According to the authors, a nonstationary and nonlinear phenomenon like the tremor may be accurately analyzed by EMD [42].

Some studies combine linear and nonlinear features for improving accuracy and obtaining more information about tremors [3], [42], [43]. Shawen et al. investigated the relationship between the characteristics estimated from the data measures and accuracy when using wearable sensor (accelerometer and gyroscope) data to classify tremor and bradykinesia in patients with PD. They selected 74 features which were categorized into the 5 feature categories (time, frequency, entropy, correlation, and derivative). They found that models monitoring tremor symptoms showed significantly decreased performance once entropy features (nonlinear) were removed, for example. They concluded that appropriate choices of features and models help to maintain accuracy. Also, the accelerometer is a sensor to detect tremors [4]. Similarly, Hssayeni et al. used a set of features estimated from a gyroscope to detect states ON and OFF medication. The specificity obtained from classifiers was over 90% [44].

Shah and colleagues conducted a study on the Hjorth parameters, which were initially proposed as a means to assess complexities present in electroencephalogram (EEG) time-series data. These complexities are not adequately captured when extracting power from different frequency bands using a wavelet transform. The authors developed a classifier that detects the presence or absence of tremor using Local Field Potentials (LPFs) recorded. They obtained an accuracy of 97% and a mean of 78% using Hjorth parameters [43][45]. Similarly, Yao et al. investigated a set of feature and machine learning methods for more accurate detection of rest tremor in PD. The authors assessed the performance of machine learning (ML) algorithms and various features of the subthalamic LFPs. The feature Hjorth complexity presented a higher correlation with tremor, compared to other features. The research concluded that the use of relevant features and learning methods improve the accuracy of tremor detection during rest [3].

In another research proposed by Yao et al., the authors using a machine learning approach for rest tremor detection from local field potentials (LFPs) recorded from the subthalamic nucleus (STN). They showed that machine learning models combined with high-frequency oscillations (HFO) and Hjorth parameters achieve a high discriminative of tremor [5].

Additionally, Hanson et al. introduced a technique frequently used in speech processing [46] for evaluating the severity of Essential Tremor. The Teager energy operator allowed to

analyze tremor at a finer level of granularity. The authors concluded that this technique offers a tremor severity metric that is accurate, precise, objective, and of higher resolution than the Clinical Rating Scale [47].

Using electromyography, some studies [6], [7], [48] suggested the presence of STMPs as a result of tremors. For instance, Dietz et al. investigated the characteristics of motor unit activity in individuals with PD. They identified three relevant patterns: rhythmic spontaneous resting discharge, abnormally low firing rates during voluntary contraction, and consistent firing patterns [7]. Similarly, Agapaki et al. focused on the detection and exploration of characteristics of motor unity (MU) synchrony and discharge patterns during rest and postural tremors [6]. Rissanen et al. also analysed differences in surface electromyography between individuals with PD and healthy subjects [48].

These results [6], [7], [48] suggest that STMPs may be linked to the underlying mechanisms that cause tremors, and they may be present in both healthy people and people with PD. STMPs exhibit self-similar structures across multiple scales of time and have a hidden dynamic with underlying structures responsible for the abnormal motion of tremors. The characterization of STMPs differs according to the type of tremor, e.g., physiological or pathological. Once a better knowledge of STMPs is achieved, such information may be used to develop better therapies and follow up on different types of pathological tremor.

According to our review of the literature, there is a lack of studies that attempt to identify and characterise STMPs in tremors, specifically using inertial sensors. Although the results reported in the literature are encouraging, with accuracies exceeding 85% for the detection of tremor during controlled tasks or free movements [4], [40], [44], [49]–[53], they do not allow for the description of several physiological phenomena that can generate and modulate STMPs over the time.

This condition was highlighted by the International Parkinson and Movement Disorder Society (MDS)[54]: “In most clinical studies, investigators are interested in changes in tremor amplitude or occurrence that exceed random variability… Currently, there is no evidence that the minimum detectable change is smaller when transducers are used.”

As a result, this study hypothesizes that tremor signals detected by inertial sensors can be used to identify STMPs. Furthermore, the appearance of STMPs is controlled by a hidden dynamic that describes their instantaneous appearance.

3.3 Short-Term Motor Patterns in tremor signals

The tremor is characterized as "a rhythmic and involuntary oscillation of a body part" [55] which is attributed to variations in time and frequency, as illustrated in Figure 3 of a real tremor signal.

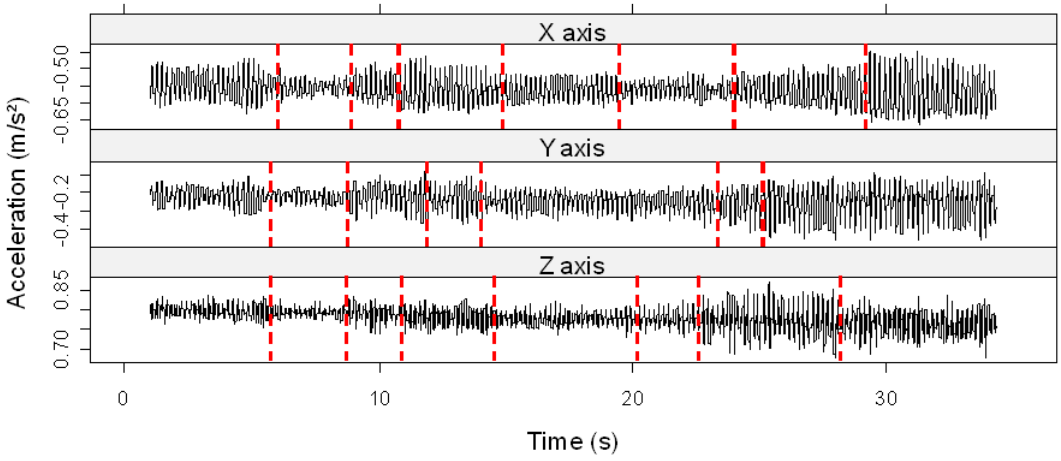

Figure 3: A signal captured by a 3-axis accelerometer sensor from an individual diagnosed with severe tremor. The red dashed line denotes the beginning and end points of the oscillations observed in the tremor signal.

These oscillations (as depicted in Figure 3) occur as a result of amplitude and frequency variations and can be regarded as an inherent variability present in the signal. This variability is characterized by the presence of short-term changes (i.e., less than 1 second) in the signals, which arise from physiological changes associated with the disorder or treatments [55]. These oscillations become more evident in more severe tremors.

In addition to the aforementioned oscillations, about 50% of patients within 2 years of initiating conventional levodopa therapy [56] experience the onset of motor fluctuations. In contrast to the short-term changes mentioned earlier, motor fluctuations are characterized by long-term variations lasting several minutes or hours [57], and they are associated with Levodopa treatment [56].

Several studies have focused on investigating the presence of long-term motor patterns, motor fluctuations, in PD [57], [58]. For instance, Erb et al. conducted a study to monitor the fluctuations in motor symptoms and complications of PD. The researchers analyzed the severity of motor symptoms in nonoverlapping intervals of 30 minutes for each participant over a period of 6 hours. They found that tremor severity changed at least twice in 67% of the 30-minute intervals examined for the upper extremities [57].

According to R. Erro et al., one of the most challenging aspects of studying tremors is dealing with within-subject fluctuations, which arise from the inherent variations in the tremor

signal over time. As most studies focused on the visible alterations in tremors (changes patterns more than 1 second or motor fluctuations), short-tremor changes, less than 1 second, cannot be captured until they exceed this natural variability [59]. In this sense, we investigated the presence of short-term motor patterns (STMPs) from inertial sensors, defined as those lasting less than 1 second, utilizing data processing tools (Figure 4).

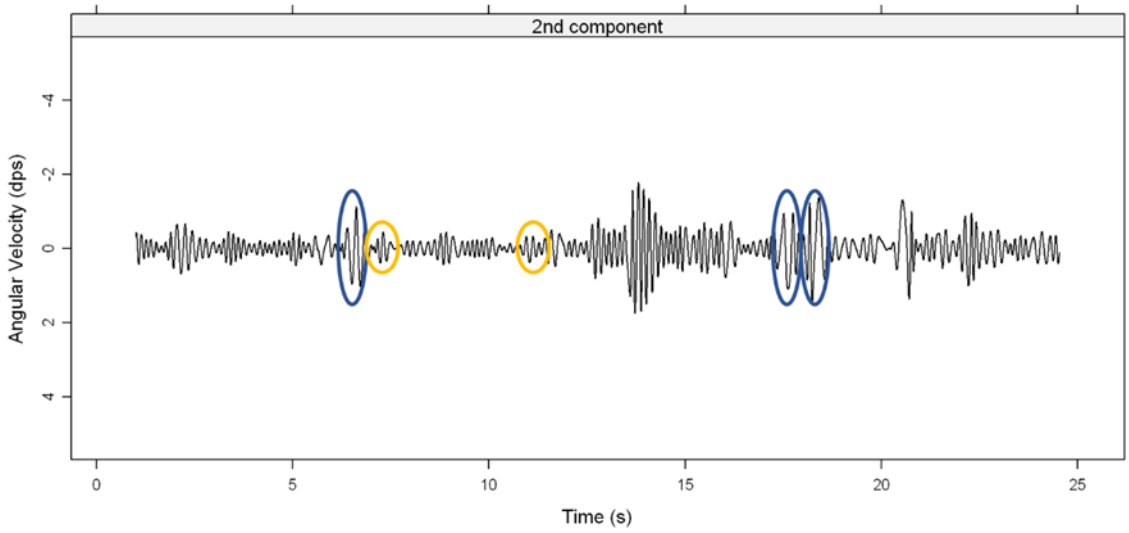

Figure 4: Second Intrinsic Mode Function estimated from X-axis gyroscope of an individual with PD. In yellow and blue circles are some examples of short-term motor patterns present in the signal.

Hand tremors, particularly, are caused by various physiological factors, such as the activity of the basal ganglia, cerebellar circuits, and peripheral nerves. These components interact at different spatiotemporal scales, contributing to the complexity of tremors. Within this intricate nature, there exists a non-random phenomenon known as STMPs (Figure 4). STMPs exhibit self-similar structures across multiple time scales and possess a hidden dynamic with underlying structures that are responsible for the abnormal movement observed in tremors.

Using electromyography, some studies [6], [7], [60] suggested the presence of STMPs as a result of tremors. For instance, Dietz et al. [7] investigated the characteristics of motor unit activity in individuals with PD. They identified three relevant patterns: rhythmic spontaneous resting discharge, abnormally low firing rates during voluntary contraction, and consistent firing patterns. Similarly, Agapaki et al. [6] focused on detecting and exploring the characteristics of motor unity (MU) synchronization and discharge patterns during rest and postural tremor. Rissanen et al. [60] also analyzed differences in electromyographic patterns between individuals with PD and healthy subjects.

According to these authors [6], [7], [60], STMPs may be linked to the underlying mechanisms that cause tremors, and STMPs may be present in both healthy people and people with PD.

The characterization of STMPs differs according to the type of tremor, e.g., physiological or pathological. Once a better knowledge of STMPs is achieved, such information may be used to develop better therapies and follow up on different types of pathological tremor.

As a result, this study hypothesizes that tremor signals detected by inertial sensors can be used to identify STMPs. Furthermore, the appearance of STMPs is controlled by a hidden dynamic that describes their instantaneous appearance. To support these hypotheses, this study aimed (i) to identify the STMPs present in resting tremor in individuals with PD and physiological tremor and (ii) to characterize STMPs in terms of amplitude, persistence, and regularity.

4. Data Collection and Exploratory Data Analysis (EDA)

In the realm of data-driven decision-making, data collection and EDA play a fundamental role in uncovering valuable insights and extracting meaningful patterns from raw data. These steps are particularly crucial in our studies aimed at identifying and characterizing short-term motor patterns of tremor signals, as there is a lack of literature on this specific content.

This section delves into the specific considerations, techniques, and tools employed in the collection and exploratory analysis of tremor data. It highlights the importance of data collection in filling the gap in the existing literature and provides an overview of the EDA methods utilized to gain insights from the collected tremor signals. Furthermore, it discusses the challenges associated with collecting and analyzing tremor data and suggests strategies to mitigate them.

4.1 Data Collection

4.1.1 Subjects

This research was approved by the Ethics Committee on Human Research (CAAE: 87716217.8.0000.5152). Inertial signals were recorded from 26 subjects. The subjects were divided into the following groups: neurologically healthy individuals (HC = 12, aged 60.1 ± 5.9 years) and individuals suffering from PD (PD = 14, aged 65 ± 11.54 years). A neurologist clinically diagnosed PD in all PD subjects. They had no evidence of dementia or musculoskeletal changes in the upper limb that were not related to PD, and they were in the ON state of medication. The ON state refers to the period when a person with Parkinson's disease experiences a significant improvement in their motor symptoms due to the effects of their prescribed medication.

The subjects with PD were recruited at the Parkinson Association of Triângulo (Associação Parkinson do Triângulo, Uberlândia, Brazil), an association for individuals with PD. Before participation in the experimental protocol, a detailed explanation was given to the participants who voluntarily signed a consent form. Table 1 summarizes the characteristics of the PD subjects.

4.1.2 Clinical evaluation

Item 21 of the Unified Parkinson's Disease Rating Scale part III (UPDRS III) was used to assess the resting tremor. The score for item 21 is based on the hand tremor at rest and ranges from 0 to 4, with 0 representing a non-visible tremor and 4 representing the most severe sign. A specialist who was not involved in the data analysis examined the PD subjects clinically. The medication was administered to the subjects between 30 and 60 minutes before the experimental protocol. The scores were assigned during the ON period of the medication. The UDPRS scores for all PD subjects are shown in Table 1.

Table 1 – Clinical evaluation of people with Parkinson's disease showing the UPDRS III scores for resting tremor on the side that is most affected.

Subject Identifier	Age	Sex	Years diagnosed with PD	Most affected side	Hand tremor at rest - Item 20 of the UPDRS
1	63	F	20	left	0
2	53	M	12	right	0
3	60	M	12	right	3
4	46	M	18	right	1
5	63	M	9	right	3
6	66	F	12	right	0
7	66	M	14	right	0
8	72	F	8	right	0
9	77	M	3	right	3
10	97	F	20	left	3
11	61	F	10	left	1
12	63	F	7	right	0
13	56	F	5	left	0
14	68	M	10	left	4

4.1.3 Experimental setup

TREMSEN (Precise Tremor Sensing Technology, National Institute of Intellectual Property—Brazil— BR 10 2014 023282 6) [61] was employed for data acquisition and real-time visualization of the two triaxial inertial measurement units (IMUS). Each IMU consists of a gyroscope unit (L3G4200D, STMicroelectronics, Switzerland) and an accelerometer–magnetometer combined unit (LSM303DLM, STMicroelectronics, Switzerland). The sensitivity settings of the IMU can be changed individually via I^2C communication.

The sensitivities of the gyroscope, accelerometer, and magnetometer were set to ± 500 degrees per second (dps) , ± 4 gravity (g), and ± 2 Gauss respectively, for all subjects, except subject 14, who had higher UPDRS scores (Table 1). Due to the high severity of the tremor of this individual the sensitivities were set to ±2000 dps, ±16 g, and±12 Gauss. All employed settings were carried out on previous studies [62], [63] and were chosen to avoid saturation of the signal conditioner. Signals were sampled at 50 Hz and digitized by a 12-bit analog-to-digital converter.

The experimental protocol used two inertial measurement units (IMUs) placed on the hand and forearm of subjects (Figure 5). Data was collected from the dominant hand of healthy subjects and from the most affected side of PD subjects.

Figure 5: The positioning of sensors in the hand during the rest task. IMU-1 placed on the hand and IMU-2 forearm.

For hand rest tremor assessment, we evaluated only recorded data from axis X of the gyroscope (IMU-1). The tremulous activity can occur in all directions, depending on limb placement and movement carried out. As the hand was in resting, the Gyroscope axis detected better the tremor. We confirmed these findings by analysing the clustering results. IMU-1 was placed on the dorsum of the hand, between the second and fourth carpometacarpal articulation (Figure 6).

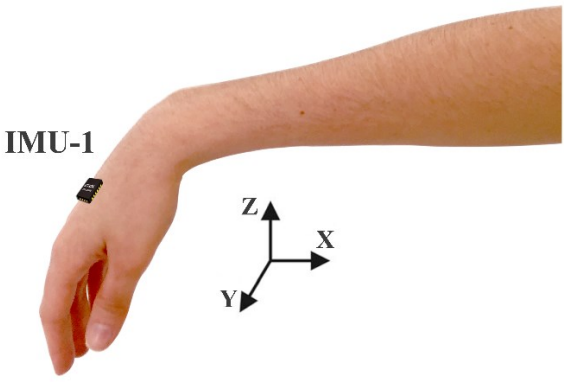

Figure 6: Illustration of the positioning of the hand during the rest tasks. The inertial sensors, IMU-1 was placed on the hand. The orientation of axes is shown, in which X, Y and Z are the proximal-distal, medial-lateral and dorsal–palmar axes, respectively.

Figure 6 presents axes orientation, in which X, Y, and Z are the proximal-distal, medial-lateral and dorsal–palmar axes, respectively.

The experiments were carried out in a room where the subject sat in a comfortable chair with an adjustable support surface. The forearm support isolated the movements of wrist joints. The subject was asked to keep the arms resting on a support surface with the hands in the free position (the shoulders at 0° and the elbow flexed at 90°), Figure 5. All subjects performed three trials. Each trial took approximately 15 s, and there was a 60 s of resting between trials.

All the data collection was organized in tables, as shown in Figure 7 that presents the general structure data collection and EDA for the identification and characterization of short-term motor patterns of tremor signals of this experiment.

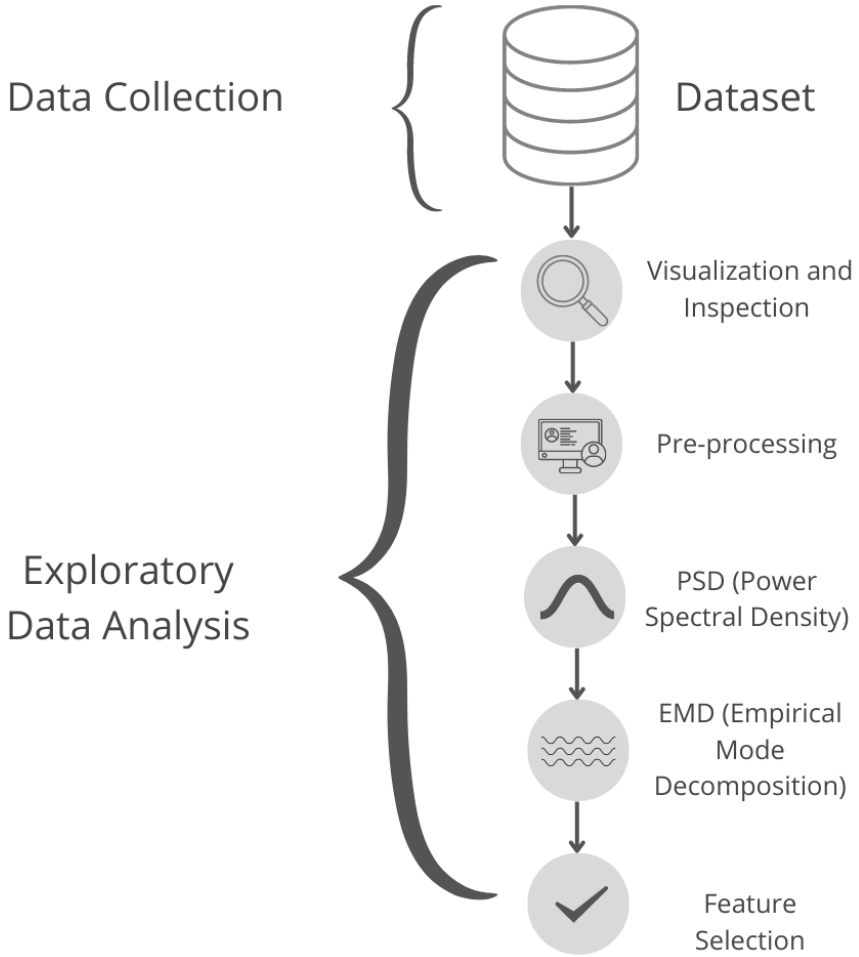

Figure 7: General structure of data collection and EDA for the identification and characterization of short-term motor patterns of tremor signals of this experiment.

Once the data has been collected, exploratory data analysis takes center stage. EDA serves as the preliminary step in understanding the inherent structure of the collected tremor data, revealing hidden patterns, and generating hypotheses for further investigation. Through the use of statistical measures, visualization techniques, and descriptive analyses, EDA helps us gain a

deeper understanding of the characteristics, trends, and potential relationships within the tremor signals [64].

4.2 Exploratory Data Analysis

The intricate diversity of tremors is likely attributed to the involvement of multiple systems and is manifested differently in individuals. STMPs are discernible in this tremor signal and their characteristics vary with tremor severity and tremor type, as pathophysiological or physiological. Understanding these subtle changes in the tremor signal, i.e., STMPs, can assist in clinical decision-making and improve the treatment of Parkinson's disease tremors.

Then, a significant question arises on how to identify and characterize these micropatterns, given that no similar study has been found. To tackle this issue, different data processing techniques were tested to develop a method for extracting STMPs.

4.2.1 Visualizing

The first stage involved understanding the dataset and signals, including those from the gyroscope, magnetometer, and accelerometer is signal visualization.

Visualizing the data is crucial for effective data processing. It allows us to gain insights into the patterns, trends, and anomalies present in the dataset. By visually examining the data, we can better understand its structure and distribution, identify potential outliers or missing values, and make informed decisions about data preprocessing techniques. Visualization helps in exploring relationships between variables, detecting patterns that might not be apparent through numerical analysis alone, and validating or refining our data processing methods[65]. Overall, data visualization enhances our ability to interpret and manipulate the data effectively, leading to more accurate and meaningful results.

Visualizing ensured data integrity and consistency for subsequent stages. In the case of the tremor signal, this step helped us gain a better understanding of tremors and the signals from various sensors. As a result, we tested multiple data processing methods that supported us in developing a protocol for identification and characterization of STMPs that will be discussed in the next sections.

We analysed and visualized all the signals, including the tremor signals captured from the gyroscope, accelerometer, and magnetometer in all axes. This comprehensive visualization, as presented in Figure 8, enabled us to identify the specific sensor and axis from which we extracted the STMPs from the tremor signal.

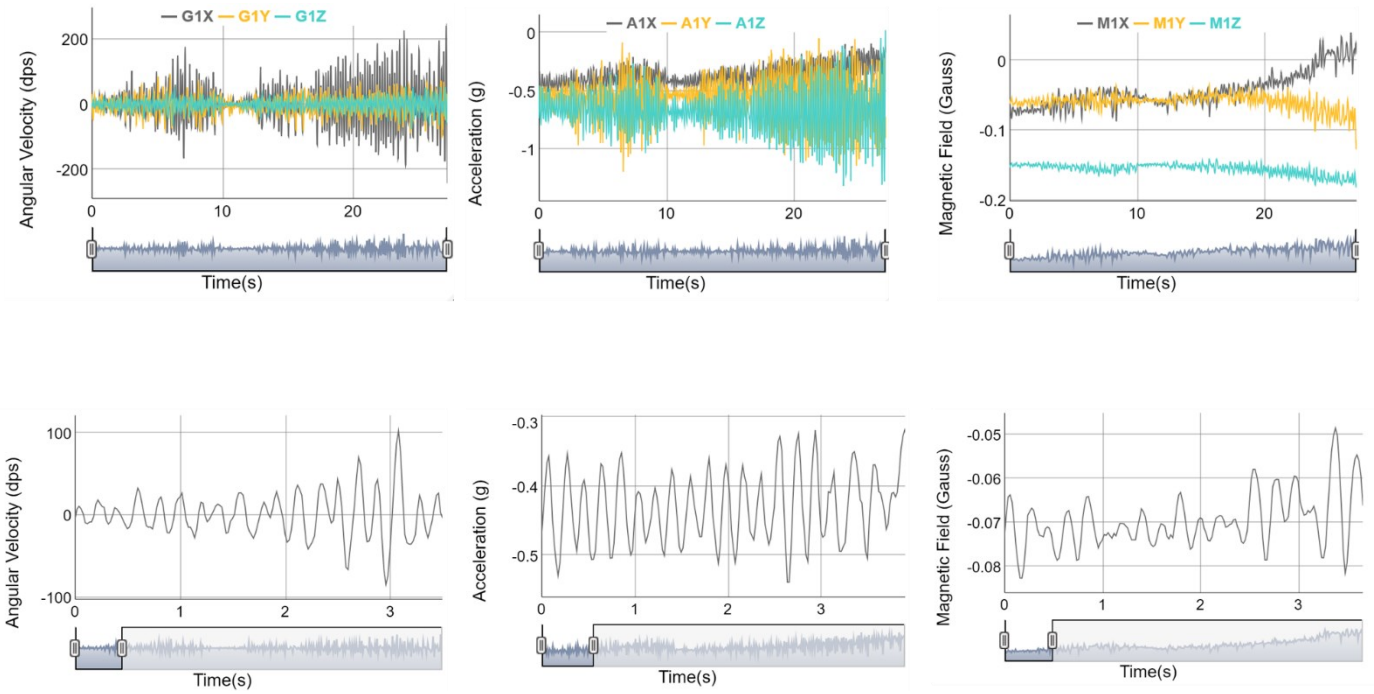

Figure 8: Raw signal captured by the gyroscope, accelerometer, and magnetometer of an individual with PD (top). At the bottom, there is a zoomed-in view of a specific section of the tremor signal along the X-axis from each of the sensors.

Visualization steps were performed at various stages of the EDA process and during data processing.

4.2.2 Signal Pre-processing

The collected signals have the influence of linear and nonlinear trends caused by various factors, including the Zero-g level offset of accelerometers, the DC component of gravity, the Earth's magnetic field, and the motion of the hand and forearm. These factors introduce low-frequency components into the signal that are unrelated to tremor [62], [63]. To address this issue, Andrade et al. [61] developed a customized toolbox which was employed in this study. This tool was utilized to eliminate both linear and nonlinear trends from the signals (Figure 9). All signal pre-processing and statistical analyses were performed using R Statistical Software. The following steps were employed for data pre-processing to identify STMPs:

- The collected data were resampled at a sampling frequency of 300 Hz using splines.
- The signals were smoothed by applying the Tukey's Running Median Smoothing (TMRS), preserving shifts in time-series. The result of this step is the smoothed signal y_{tmrs}.

- Following that, the low-frequency components related to involuntary movements not related to the tremor, and linear trends from the signals were detected, using the Loess Regression with the neighbourhood of size 0.1. The nonlinear slow component y_{loess} was obtained.
- Nonlinear component was removed from the smoothed signal to obtain:
  $y_r = y_{tmrs\_} y_{loess}$
- The last step removes the piecewise linear trend y_d using the detrend function from the *pracma* package. y_d is a detrend signal and it will be employed for data processing.

These signal processing steps are fully explained in [61]. In cases where the outliers were not removed during the initial step of data pre-processing, we utilized box plots to detect them and subsequently removed them from the dataset.

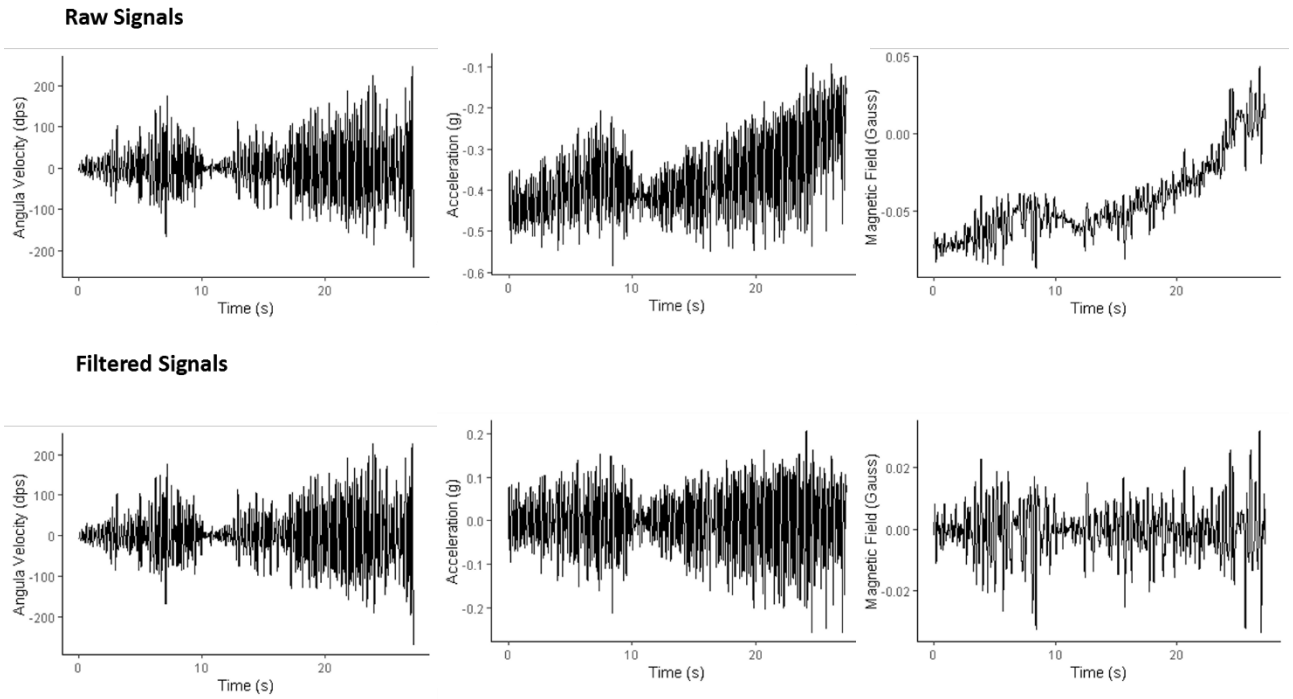

Figure 9: Raw signals captured by X-axis from gyroscope, accelerometer, and magnetometer of an individual with PD (top). At the bottom, filtered the Y-axis signals from each of the sensors.

4.2.3 Power Spectral Density (PSD)

Moreover, to understand better the signals, we estimated the power spectral density (PSD) of all the signals (Figure 10) through the Adaptive Sine Multitaper method as described in [66]. In this method time-series data are divided into multiple equal length segments. A set of orthogonal "taper" functions are multiplied with each segment of the time-series data before

obtaining the periodograms. The average of all segmented periodograms is the tapered version of the time-series data. This two-step multiplication and average process can reduce the spectral leakage in the PSD, thus lowering the variance and bias relative to the standard Fourier transform. The psd package, available in The R Project for Statistical Computing [67], was used to estimate the PSD (Figure 10).

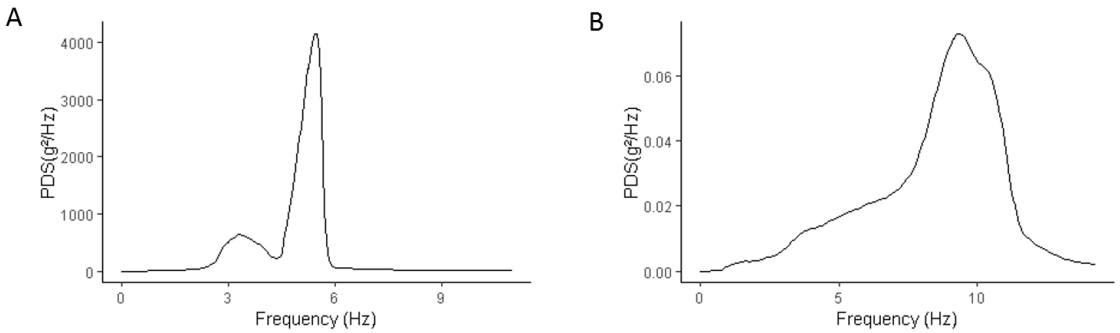

Figure 10: Power Spectral Density (PDS) estimated from the X-axis of the Gyroscope. On the left side (A), the PDS is estimated from an individual with Parkinson's disease (PD), while on the right side (B), the PDS is estimated from a healthy individual.

As observed in Figure 10 (A), the PDS exhibits peaks at lower frequencies (3-5 Hz) with higher energy in individuals with Parkinson's disease. In contrast, for a healthy individual (Figure 10 - B), the peak is within the range of (5-10 Hz) with lower energy, which is consistent with findings reported in the literature [31], [68]. In this case, it is easier to detect and distinguish Parkinson's tremor from a physiological tremor. This is due to the PDS estimated in Figure 10 (A) being derived from an individual with a tremor level of 4 (severe) according to MDS-UPDRS. This indicates a signal with higher amplitude and more regularity, as illustrated in Figure 11.

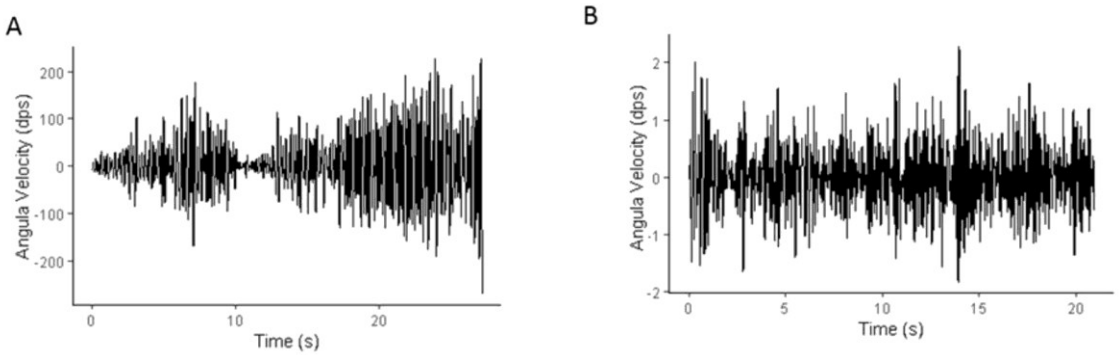

Figure 11: The pre-processed signal from the X-axis of the Gyroscope. On the left side (A), the signal is from an individual with Parkinson's disease (PD), while on the right side (B), the signal is from a healthy individual. These signals were used to estimate the Power Spectral Densities (PDS) shown in Figure 10.

In contrast, distinguishing individuals with slight to moderate Parkinson's tremor from physiological tremor solely using the PDS becomes more challenging. This is due to the frequency overlap between physiological tremor and Parkinson's tremor, as well as the similarity in energy levels to signals from healthy individuals (Figure 12).

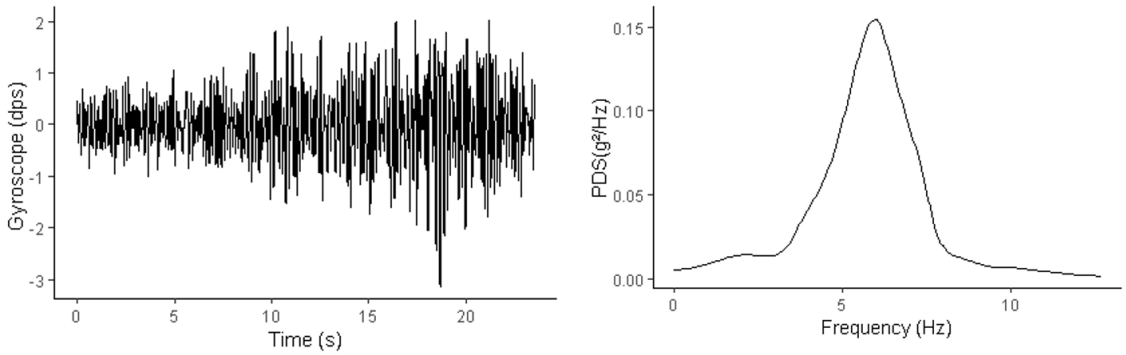

Figure 12: On the left side, there is a moderate tremor signal from an individual with Parkinson's disease (PD), while on the right side, there is a Power Spectral Density (PDS) estimated from this signal.

In contrast to Figures 10 and 11 (A), the tremor signal depicted in Figure 12 exhibits a lower amplitude, and the frequency peak falls within the range of (5-9 Hz), resembling tremor signals commonly observed in healthy individuals. Traditional methods may not be sufficient to detect and differentiate slight and moderate tremors from psychological tremors. Therefore, we investigated on an exploration of methods capable of revealing hidden structures to effectively distinguish between these types of tremors. As part of our investigation, we utilized Empirical Mode Decomposition (EMD) to analyze the tremor signal.

4.2.4 Empirical Mode Decomposition (EMD)

As mentioned earlier, tremor is a complex signal, and detecting and differentiating slight and moderate tremors can be challenging. Numerous tools and protocols have been developed to address this issue. However, many of these methods assume that tremor is linear and stationary, for instance, the Fourier transform (FT) [69]. Methods based on FT are commonly employed for tremor analysis. However, using FT for tremor analysis has some drawbacks. Firstly, the signal is linearly decomposed as a combination of sines and cosines, which may not fully capture its complexity. Additionally, methods based on FT often face a trade-off between time and frequency resolution, which can hinder the detection of local oscillations in the signal that may have significant physical meaning [41], [70], [71].

In this context, we employed EMD for identifying hidden structures in tremor signal, as this technique provides enough resolution in the signal analysis to detect events often obscured in conventional analysis. EMD technique for analysis of nonlinear and nonstationary time-series

was successfully applied to investigations of seismological and biological signals, including tremors [70], [72], [73].

This method decomposes the input time-series into a finite and often small number of functions designated as Intrinsic Mode Functions (IMFs) [74]. IMF represents the oscillation modes embedded in the data, unlike the Transform Fourier, which breaks down signals in terms of sine and cosine waves.

An IMF satisfies two conditions:

- First, in the whole data set, the number of extrema and the number of zero crossings must be either equal or differ at most by one.
- Second, at any point, the mean value of the envelope defined by the local maxima and the envelope defined by the local minima is zero.

The main aim of the EMD is to iteratively identify distinct timescales (or frequency bandwidths) from the data that may have a physical meaning, e.g., IMFs may be related to biological phenomena.

To identify a specific Intrinsic Mode Function (IMF) associated with the tremor, we estimated five IMFs and examined the PSD of each IMF. The selection of the IMF was based on the presence of oscillations within the frequency range of 3 Hz to 10 Hz, which is known to be associated with tremors [70].

Through this analysis, we have discovered the presence of short patterns in the tremor signals, and it is likely that these short patterns contribute to the diverse manifestations of tremors. Figure 13 illustrates some of these short patterns observed in two different tremor signals.

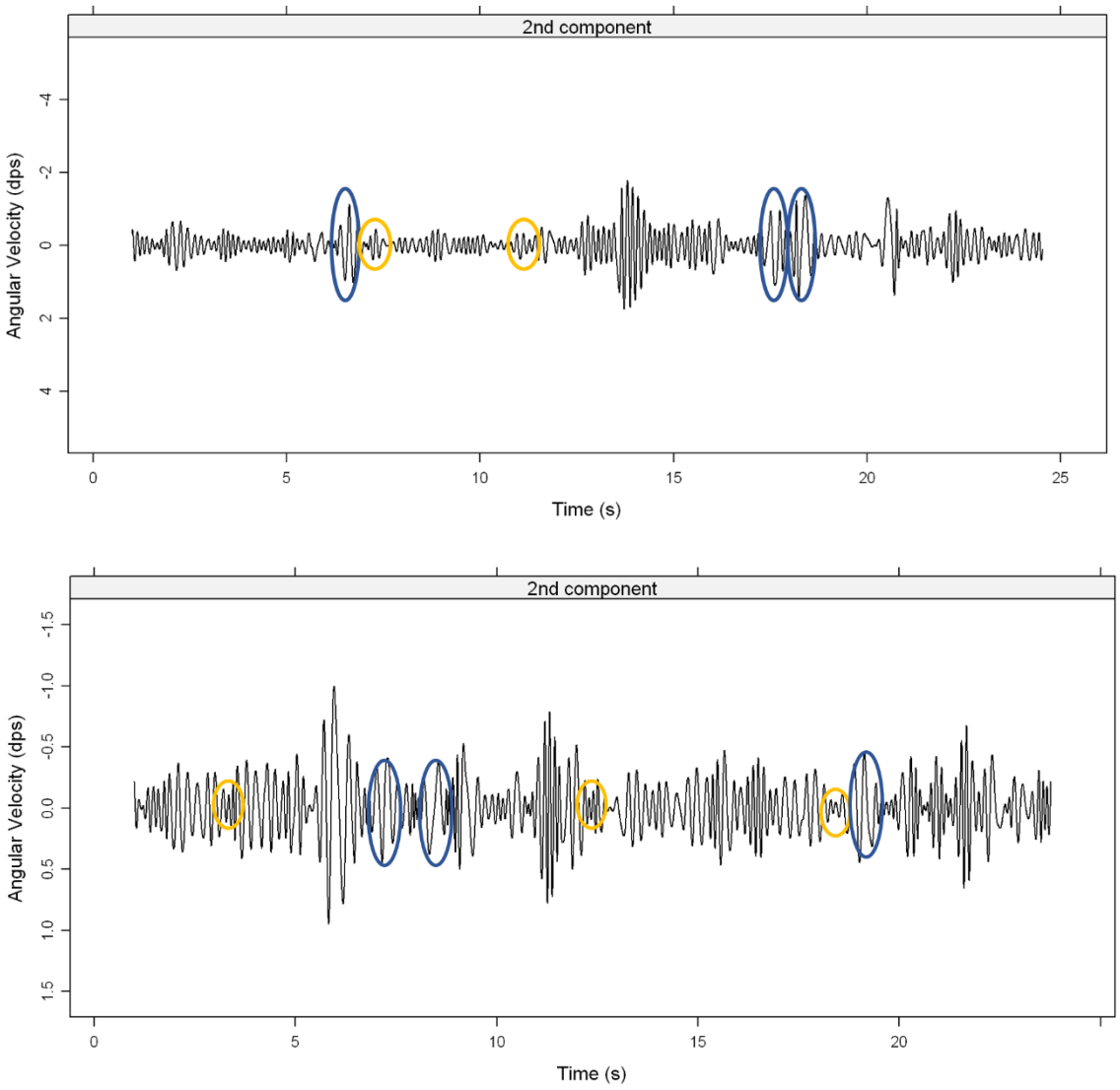

Figure 13: The Y-axis gyroscope was used to estimate the second IMF of two different signals. Some of the short patterns identified through visual inspection are represented in yellow and blue.

Through visual inspection (Figure 13), several insights about tremors have emerged:

- Due to the nonlinear nature of the signal, it is necessary to combine both linear and nonlinear features to effectively characterize tremor signals.
- According to a study by Andrade et al. [61] , tremors can occur in various directions and exhibit variations based on the level and type of tremor. Because of that, the X-axis of the gyroscope suggests providing additional information about tremors. Additionally, the choice of the IMF component with a physical meaning depends on the severity of the tremor. For mild or moderate tremors, the second and first components are more representative, while for more severe tremors, the third component is a suitable choice. Similar findings have been reported in the literature [42], [70].

- The instantaneous appearance of short patterns follows a specific dynamic.

To uncover the patterns present in the tremor signal, we conducted an investigation focusing on the features that can be extracted from the X-axis of the gyroscope. The purpose of this analysis was to explore and understand the specific characteristics and patterns exhibited by the tremor signal along the X-axis.

4.2.5 Feature Selection

The selection of appropriate features can significantly impact the performance of a data analysis. Relevant features provide valuable information and can lead to more accurate predictions, classifications, or insights.

Considering the nonlinearity and nonstationary of tremor signals, a more robust approach to this analysis involves selecting features that combine linear and nonlinear characteristics [69]. By incorporating both types of features, a more comprehensive and complementary set of information can be obtained from hand tremor signals [75]. Based on these premises and literature, we investigated a set of features in time domain for identification and characterization of STMPs in tremor signals [3], [5], [69], [75].

The amplitude of tremor plays a crucial role in characterizing its severity. Many studies evaluating tremor employ features that are derived from the amplitude of the tremor signal [3], [5], [61], [69], [75], including the use of this criterion in MDS-UPDRS to evaluate the severity tremor [76]. Also, features related to randomness can be useful to bring news insights about the tremors. They are applied for determining the regularity of series of data based on the existence of patterns [77].

Additionally, we opted to utilize features in the time domain due to their ability to preserve the temporal information of the signal, offering valuable insights into the dynamics and temporal changes over time. This is especially crucial when analyzing time-varying signals like tremors, as it allows for a better understanding of temporal patterns and variations. Moreover, time domain features involve simpler calculations compared to frequency domain features, making them faster and computationally less demanding. This efficiency makes time domain features well-suited for real-time or large-scale data processing tasks.

We selected this set of features for identification and characterization of STMPs in tremor signals: mean absolute value (MAV), coefficient of variation (CV), zero crossing rate (ZCR), sample entropy (SampEn), and Hjorth parameters (activity-ACT, mobility-MOB, complexity-COMP).

4.2.5.1 Mean Absolute Value (MAV)

Mean Absolute Value (MAV) is a feature commonly used in the analysis of physiological signals, particularly in the field of electromyography (EMG) [78]. It quantifies the average magnitude of the signal by calculating the mean of the absolute values of the amplitude of the signal over a specific time window (Equation 1).

$$MAV = \frac{1}{N}\sum_{i=1}^{N} |x_i| \tag{1}$$

Considering N is the total number of samples of the discrete time-series x of each window, i is the *i-th* discrete time instant (i={1,2,3,⋯,N}).

MAV is a simple and widely used feature that can be useful for various applications, such as muscle activity monitoring, gesture recognition, or movement analysis [79], [80].

4.2.5.2 Coefficient of Variation (CV)

Coefficient of Variation is a statistical measure that expresses the relative variability or dispersion of data. The CV is commonly used to compare the variability of different data. It allows for a standardized comparison of variability relative to the mean. A higher CV indicates a greater degree of relative variability or dispersion in the data, while a lower CV suggests more consistent or stable data (Equation 2).

$$CV = \frac{\sigma(x)}{\mu(x)} \tag{2}$$

Considering N is the total number of samples of the discrete time-series x of each window, i is the *i-th* discrete time instant (i={1,2,3,⋯,N}), μ is the mean and σ the standard deviation of x.

The CV is often used in various fields, including finance, economics, biology, and quality control, to assess and compare the relative variability of different variables or measurements [81], [82]. It provides a useful measure for understanding the spread or dispersion of data in relation to the mean.

4.2.5.3 Zero Crossing Rate (ZCR)

Zero Crossing Rate is a feature commonly used in the analysis of audio, speech, and biomedical signals[3], [83]. It represents the rate at which a signal crosses the zero-axis over a given period of time (Equation 3).

$$ZCR = \frac{1}{2N}\sum_{i=1}^{N} |sgn(x_{i+1}) - sgn(x_i)| \tag{3}$$

Considering N is the total number of samples of the discrete time-series x of each window, i is the i-th discrete time instant (i={1,2,3,⋯,N}), μ is the mean and σ the standard deviation of x.

The ZCR provides information about the rate of changes or transitions in the signal and is particularly useful in characterizing the temporal properties. Signals with a higher ZCR tend to have more rapid changes in amplitude or frequency, indicating a more dynamic signal. On the other hand, signals with a lower ZCR tend to have smoother or more stationary characteristics.

4.2.5.4 Sample Entropy (SampEn)

Entropy is a nonlinear technique rooted in the theory of complex systems, serving to quantify the randomness and predictability of stochastic processes[84]. In clinical monitoring, different forms of entropy have been employed. One such measure is Sample Entropy (SampEn), which assesses regularity. It is computed as the negative natural logarithm of the conditional probability that two sequences (Equation 10), sharing similarities for a specified number of points, will continue to exhibit similarities at the subsequent point, with the exclusion of self-matching. Considering N is the total number of samples of the discrete time-series x of each window, i is the *i-th* discrete time instant (i={1,2,3,⋯,N}). SampEn of the time series can be calculated as follows:

- Construct an embedding vector with m consecutive data points extracted from x: $v_i = [x_i,\ x_{i+m}, \dots, x_{i+m-1}]$, and m is the embedding dimension
- Define for each i ($1 \le i \le N - m$)

$$C_i^m = \frac{1}{N-m-1}\sum_{j=1,j\neq i}^{N-m} \Theta(r - ||v_i - v_j||). \quad (4)$$

r specifies a tolerance value and $r = \varepsilon\sigma_x$ where ε is a scaling parameter and σ_x is the standard deviation of x.

- Θ(·) is the Heaviside function:

$$\Theta(x) = \begin{cases} 0, x < 0, \\ 1, x \ge 0 \end{cases} \quad (5)$$

- $\|\cdot\|_1$represents Chebyshev distance, that is,

$$\| v_i - v_j \|_1 = \max\left(|x_i - x_j|, |x_{i+1} - x_{j+1}|, \dots, |x_{i+m-1} + x_{j+m-1}|\right). \quad (6)$$

- C_i^m represents the proportion of v_j ($j \neq i$) whose distances to v_i are less than r. Similarly, for each i ($1 \le i \le N - m$), we also define

$$C_i^{m+1} = \frac{1}{N-m-1}\sum_{j=1,j\neq i}^{N-m} \Theta(r - ||v_i - v_j||). \quad (7)$$

where C_i^{m+1}represents the proportion corresponding to the dimension of $m + 1$; C_i^m and C_i^{m+1} have the same form, but embedding vectors in the two cases are defined in different phase spaces.

- Averaging across all embedding vectors

$$A = \frac{1}{N-m-1}\sum_{i=1}^{N-m} C_i^m \tag{8}$$

- And

$$B = \frac{1}{N-m-1}\sum_{i=1}^{N-m} C_i^{m+1} \tag{9}$$

SampEn of x is calculated as

$$SampEn(m,r,N) = -log\frac{A}{B} \tag{10}$$

According to Equation 10 a lower SampEn value indicates a higher degree of self-similarity in a given time series. For this application, we adopted $m = 2$ and $r = 0.2$ based on previous studies [44], [83].

SampEn has demonstrated its efficacy as a valuable tool for examining diverse types of time series data originating from various biological conditions within the human body, such as Alzheimer's disease, Parkinson's Disease, and human postural sway[85]–[87].

4.2.5.5 Hjorth parameters

In 1970, Hjorth introduced a set of three descriptors to evaluate the EEG signal in the time domain [88]. These descriptors rely on the signal's variance, offering a computationally efficient alternative compared to other time-frequency methods like Fast Fourier Transform (FFT) and wavelets [88], [89].

As described by Hjorth, the first parameter, known as activity, represents the average power of the signals. The second parameter, mobility, indicates the mean frequency of the signal. The third parameter, complexity, characterizes the shape of the signal's curve. For instance, the complexity value of a pure sine wave converges to one. Hjorth combined these three parameters for characterizing the patterns of EEG signals related to amplitude, the scale of time, and complexity in the time domain [88].

Activity (ACT)

Activity provides a measure of the squared deviation of the amplitude (Equation 11)

$$Activity = \sigma_a^2 \tag{11}$$

Mobility (MOB)

Mobility provides a measure of the standard deviation of the slope concerning the standard deviation of the amplitude (Equation 12)

$$Mobility = \frac{\sigma_d}{\sigma_a} \tag{12}$$

Complexity (COMP)

Complexity gives us the number of standard slopes obtained through the average time required for generation of one standard amplitude (Equation 13)

$$Complexity = \frac{\frac{\sigma_{dd}}{\sigma_d}}{\frac{\sigma_{dd}}{\sigma_a}} \tag{13}$$

In addition to EEG signals, the Hjorth Parameters are also used for gait analysis and tremor analysis in Parkinson's disease (PD) [3], [88], [89].

Although the results reported in the literature regarding the utilization of the aforementioned features are promising, they do not provide a comprehensive understanding of how these descriptors behave in various data collection scenarios. This is particularly evident in the case of tremor, which is a complex signal characterized by trends, frequency variations, and amplitude variations. These factors can potentially impact the outcomes of the estimated features. Therefore, characterizing the behavior of these features in different scenarios is essential for gaining a deeper understanding of the results. One method commonly employed to assess their behavior is by utilizing synthetic signals [71], [90], [91].

4.2.6 Synthetic Signals

Synthetic signals, also known as artificial signals or simulated signals, are artificially generated signals that mimic or emulate real-world signals. They are created based on mathematical models, algorithms, or predefined patterns to possess specific characteristics and properties. Synthetic signals are designed to resemble the properties and behavior of real signals, allowing researchers to study and analyze them in a controlled and systematic manner [91].

Synthetic signals are often used in various fields, including signal processing, machine learning, and data analysis. They serve as valuable tool for evaluating algorithms, testing methodologies, and understanding the behavior of different systems. By generating synthetic signals, researchers can manipulate various parameters, such as frequency, amplitude, noise, and

time-varying characteristics, to investigate the effects of these factors on data processing methods and algorithms [90].

The advantages of using synthetic signals include the ability to establish ground truth, control over signal characteristics, reproducibility, and the ability to perform controlled experiments. Synthetic signals provide a standardized basis for evaluating algorithms, comparing different methods, and validating the performance of data processing techniques [90], [91].

In the context of tremor analysis, synthetic signals can be generated to mimic the characteristics of tremor signals, including their frequency, amplitude, and noise properties. These synthetic signals can then be used to evaluate the effectiveness of feature extraction algorithms, assess the impact of different factors on the extracted features, and explore the underlying mechanisms of tremor.

Overall, synthetic signals play a crucial role in research and development by providing researchers with controlled and reproducible signals that enable deeper insights and advancements in various fields, including data processing and analysis. Therefore, based on synthetic signals, we explored the behavior of the set features (MAV, ZCR, SampEn, and Hjorth parameters) in different five scenarios of data collection.

In theoretical terms, tremor can be simulated by summing sinusoidal signals and by multiplying sinusoidal frequencies that are different from the ones used in the sum, as described in [92]. However, for the purpose of this study, we chose to simulate a single sine wave with different parameters (i.e. amplitude, frequency, noise, and trends) to gain a better understanding of the applied set of features. The sine wave is commonly employed in biomedical signal studies because of its similarity to the shape of a sinusoid, which is frequently observed in various biomedical signals, including tremor [93], [94]. Additionally, the behavior of the sine wave is well-established, making the analysis simpler and more controlled [92].

The assessment of these features was carried out from the sine wave. The Equation (4) describes this sine:

$$y\,(t) = A sin(2\pi f t) \tag{12}$$

Where:

y (t): Sine wave, A: Amplitude, *f:* Frequency (Hz), and *t:* Time (s)

1) First scenario

To observe the sensitivity of features according to the amplitude. The amplitude (A), Equation (12), varied among different values, A_1 = 0.5, A_2 = 0.55, and A_3 = 5. For the different amplitudes, we considered f = 3 Hz, and sampling rate f_s = 50 Hz. Figure 14 shows the artificial signal considering f = 3 Hz, A_1 = 0.5, and f_s = 50 Hz.

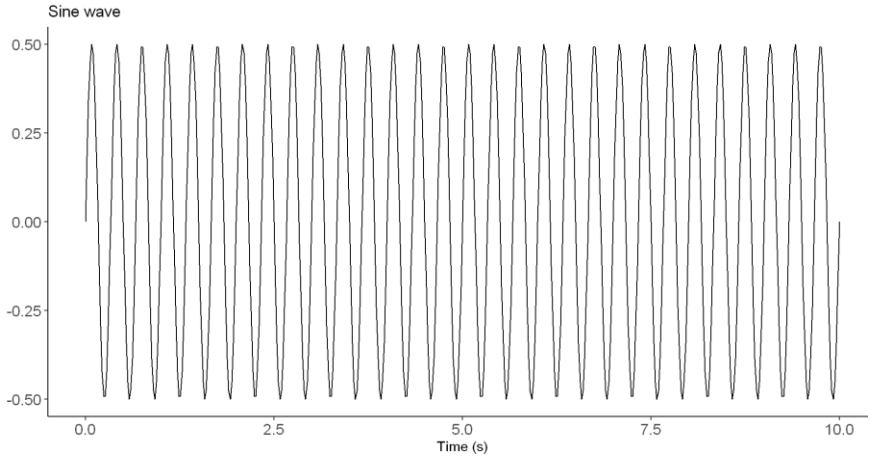

Figure 14: Pure sine wave with amplitude 0.5.

Results from the first scenario

Table 2: Results of features according to the amplitude

Amplitude	MAV	ZCR	sampEn	ACT	MOB	COMP
0.5	0.32	0.12	0.005	0.13	18.76	1.00
0.55	0.35	0.12	0.005	0.15	18.76	1.00
5	3.17	0.12	0.005	12.5	18.76	1.00

Comments

The variables related to amplitude, such as MAV and ACT were found to be sensitive to even small variations in amplitude, such as 0.05. On the other hand, the variables related to the shape and regularity of the signal remained unchanged, indicating that they were not affected by amplitude variations.

2) Second scenario

To observe the sensitivity of features according to the frequency. We varied f in Equation (12) among different values: f_1 = 3 Hz, f_2 = 5 Hz, and f_3 = 10 Hz. For the different frequencies we considered A = 0.5, and sampling rate f_s = 50 Hz. Figure 15 shows the artificial signal considering f = 5 Hz, A = 0.5, and f_s = 50 Hz

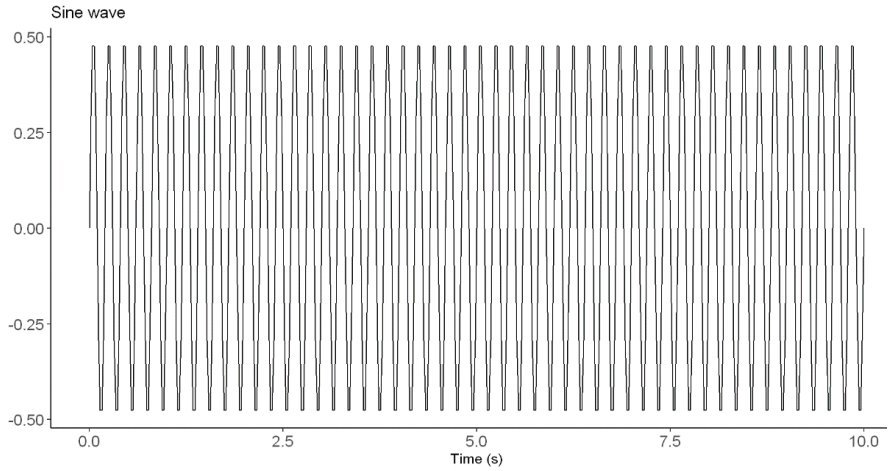

Figure 15: Pure sine wave with frequency 5 Hz.

Results from the second scenario

Table 3: Results of features according to the frequency

Frequency	MAV	ZCR	sampEn	ACT	MOB	COMP
3	0.32	0.12	0.005	0.13	18.76	1.00
5	0.31	0.20	0.004	0.13	30.93	1.00
10	0.31	0.40	0.004	0.13	58.84	1.00

Comments

The variables related to frequency in time domain, such as ZCR and MOB were found to be sensitive variations in frequency. The feature related to variability of the signal, CV, also was sensitivity. On the other hand, the variables related to the amplitude, shape and regularity of the signal remained unchanged, indicating that they were not affected by frequency variations.

3) Third scenario

To observe the sensitivity of features according to addition of the white noise. We considered A = 0.5, f = 5 Hz, and sampling rate f_s = 50 Hz. Figure 16 shows the sine wave contaminated with white noise.

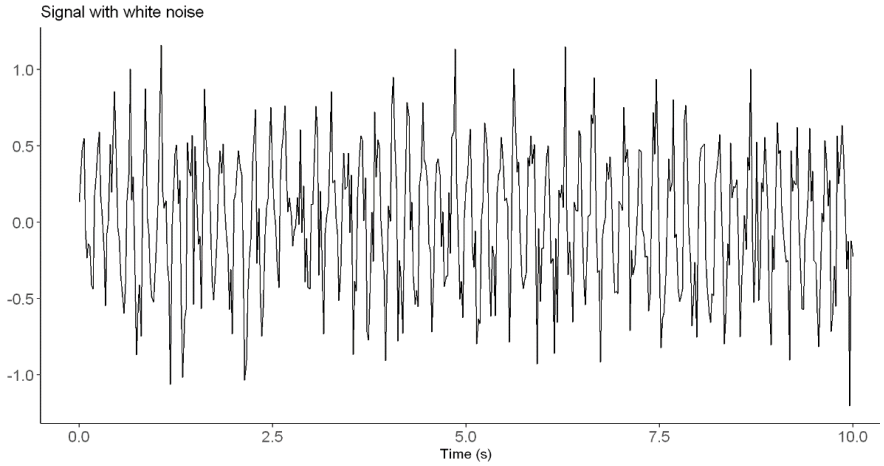

Figure 16: Sine wave contaminated with white noise.

Results from the third scenario

Table 4: Results of features according to the addition of white noise

MAV	ZCR	sampEn	ACT	MOB	COMP
0.37	0.25	1.9	0.20	48.79	1.56

Comments

All the variables were found to be sensitive to the addition of white noise. However, the variables related to frequency in the time domain and regularity were particularly affected, showing the greatest impact.

4) Fourth scenario

To observe the sensitivity of features according to addition of the linear trend. We considered A = 0.5, f = 5 Hz, and sampling rate f_s = 50 Hz. Figure 17 shows the sine wave with linear trend.

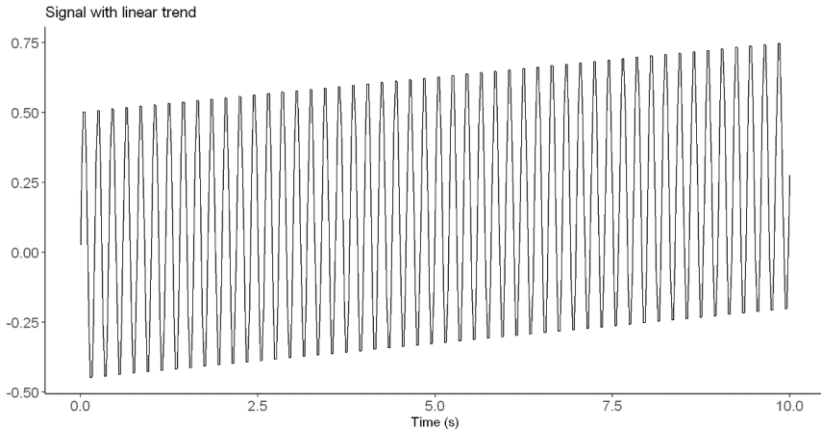

Figure 17: Sine wave contaminated with linear trend.

Results from the fourth scenario

Table 5: Results of features according to the addition of linear trend

MAV	ZCR	sampEn	ACT	MOB	COMP
0.34	0.20	0.008	0.13	30.39	1.01

Comments

All the variables were found to be sensitive to the addition of linear trend. However, the variables related to frequency in the time domain and regularity were particularly affected, showing the greatest impact.

5) Fifth scenario

To observe the sensitivity of features according to addition of the nonlinear trend. We considered A = 0.5, f = 5 Hz, and sampling rate f_s = 50 Hz. Figure 18 shows the sine wave with nonlinear trend.

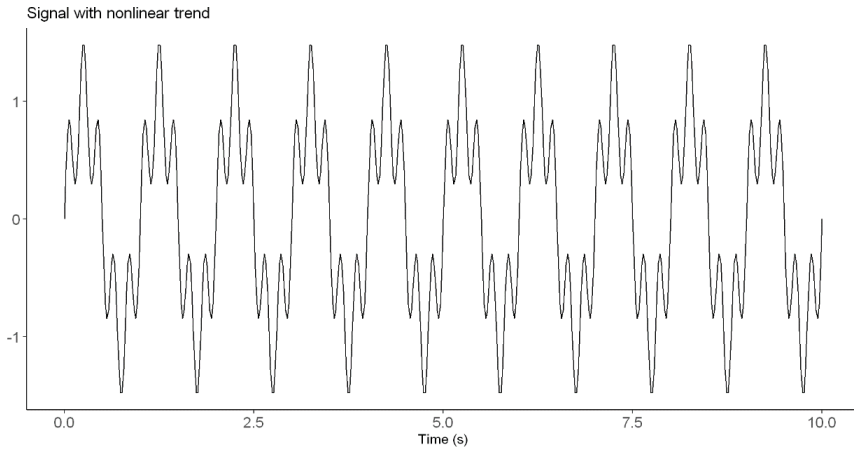

Figure 18: Sine wave contaminated with nonlinear trend.

Results from the fifth scenario

Table 6: Results of features according to the addition of nonlinear trend

MAV	ZCR	sampEn	ACT	MOB	COMP
0.70	0.04	0.45	0.63	14.93	1.93

Comments

All the variables were found to be sensitive to the addition of nonlinear trend.

5. Protocol for identification and characterization of STMPs

After conducting an explanatory analysis of the data, we concluded that the X-axis data from the gyroscope holds crucial information regarding short-term patterns. The tremor was more evident in the gyroscope X-axis than other sensors. Subsequently, we proceeded to follow the flow outlined in Figure 19 to identify and characterize STMPs.

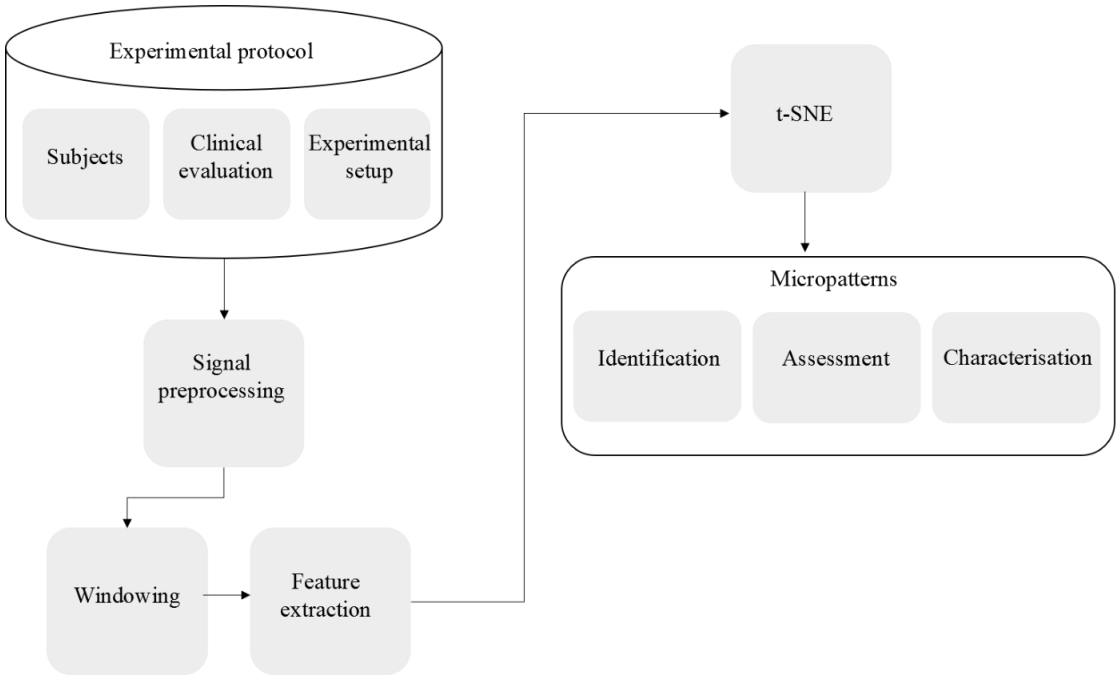

Figure 19: Diagram depicting the main steps for the identification and characterization of STMPs.

The Experimental protocol and signal pre-processing were detailed on the previous sections. After these steps, we developed a protocol for identification and characterization of STMPs as shown in Figure 19.

5.1 Windowing and feature extraction

Prior to feature extraction, the signals were divided into 1 s windows with 50% overlap (Figure 20). To identify the STMPs in the signal, the following linear and nonlinear features were extracted from each window: MAV, CV, ZCR, sampEn, and Hjorth parameters (activity-ACT, mobility-MOB, complexity-COMP), as defined in previous section and APPENDIX A. As a result of the feature estimation, the data in each signal window were represented by a feature vector of dimension seven.

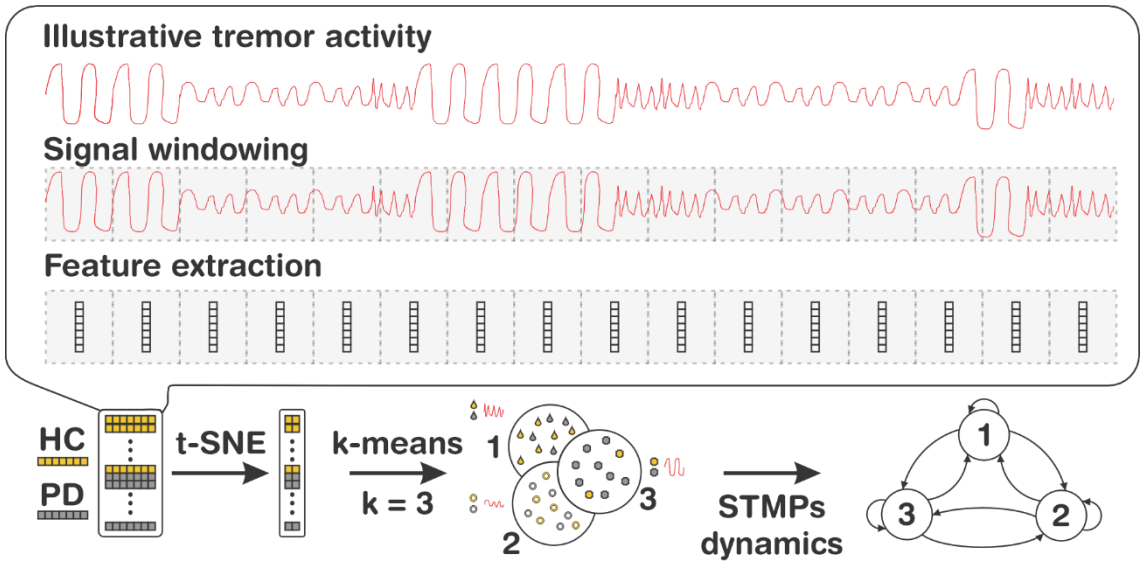

Figure 20: The main steps in tremor data analysis of healthy individuals (yellow) and individuals with PD (gray). The tremor activity may have distinct STMPs that emerge over time. The signal is windowed, and a feature vector is estimated for each overlapping window delimited by the arrows. Black and red colors are used to ease the visualization of the boundaries of each window. The set of features is estimated for individuals in the HC and PD groups. The high-dimensional data set is reduced to a lower-dimensional space using t-SNE, allowing the identification of clusters representing distinct STMP (represented by numbers 1, 2, and 3) templates present in the tremulous activity. Once these STMP groups have been identified, it is possible to understand their dynamics over time, i.e., the likelihood of STMP appearance, persistence, and regularity.

The primary goal of this study was to detect STMPs and characterize them using the studied time domain features. Although these features are estimated in time, some of them (ZC and Mobility) capture changes in signal frequency. In this sense, the set of features chosen combines the features capable of capturing information about changes in the frequency, amplitude, and predictability of the signals.

5.2 Dimensionality reduction

The dimensionality of the data, i.e., feature vector, was reduced through t-Stochastic Neighborhood Embedding (t-SNE) [95], which converts data in a high-dimensional space into a low-dimensional space while preserving the stochastic distribution of data points. The data was standardized by using the zscore method before the dimensionality reduction.

t-SNE is a nonlinear method that converts the high dimensional data set $X = \{x_1, x_2, x_3, \dots, x_n\}$ two- or three-dimensional data $Y = \{y_1, y_2, y_3, \dots, y_n\}$. The low-dimensional data Y is represented as a map, while the low-dimensional representations y_i of individual data points as map points. The SNE algorithm converts Euclidean distances between high-dimensional data points into conditional probabilities (p_{ij}, and q_{ij}). The pairwise similarities between two

datapoints, x_i and x_j, are represented by the conditional probability p_{ij} in the original high-dimensional space, and the low-dimensional conditional probability is represented by q_{ij} of points y_i and y_j. For nearby datapoints, p_{ij} is relatively high, whereas for widely separated datapoints, p_{ij} will be almost infinitesimal.

In order to determine how much the low-dimensional model represents well the high-dimensional model, the t-SNE minimizes the Kullback Leibler (KL) [95] cost function using a gradient descent method (Equation 13)

$$C = \sum_i KL(P_i||\mathrm{Q}i) = \sum_i \sum_j p_{ij} log \frac{p_{ij}}{q_{ij}} \tag{13}$$

Where P_i is the conditional probability distribution over all data points given a data point xi and Q_i represents the conditional probability distribution over all other map points given map point y_i. The location of the points y_i in the map is defined by minimizing the KL divergence of the distribution P from the distribution Q. The goal is to optimize the embedding such that p_{ij} and q_{ij} are as similar as possible. t-SNE improves SNE by using the Student's t-distribution rather than a Gaussian to compute the similarity between two points in the low-dimensional space [95].

The perplexity parameter in t-SNE determines the point's optimal number of close neighbours. Van der Maaten and Hinton [95] suggest values between 5 to 50. However, due to the number due to the number of points from our sample, the algorithm did not properly work with perplexity values higher than 15. Then, we ran some experiments with perplexity values in the range between 5 and 15 to verify how this parameter affected the quality of the generated maps. With the map generated by t-SNE, we observed that the perplexity values smaller than 10 generated a large number of clusters dominated by local variations. In contrast, with perplexity values higher than 10, the number of clusters was reduced. Based on this, the perplexity value was set to 10.

5.3 Identification of STMPs

STMPs were identified for the HC (healthy control) and PD (Parkinson's disease) groups using the k-means clustering technique applied to the data in a two-dimensional space created by t-SNE. To determine the optimal number of clusters for the dataset, the gap statistic [96] and Silhouette plot [97] were utilized, estimating the optimal number as 3. Despite testing other values of k, including $k = 2$, 4, 5, and 6, a cluster value of $k = 3$ (Figure 22) provided the most meaningful

interpretation of the presence of STMPs in the signals. Prior to clustering, all variables were transformed into z-scores.

In addition, differences between pairwise clusters were evaluated using the Fasano–Franceschini test [98] ($p < 0.05$) because the bivariate normal distribution assumption of the variables was violated (Kolmogorov–Smirnov test at the significance level of 5%).

5.3.1 STMPs assessment

The frequency of the STMPs in each group, the transition probability among the STMPs in each group, and the time duration of the STMPs in each group were all evaluated. The transition probability among the STMPs was calculated based on the transition probability matrix denoted as P, which contains all transition probabilities. Assuming the states are 1,2, …, r, then the state transition matrix is given by

$$P = \begin{bmatrix} p_{11} & \cdots & p_{1r} \\ \vdots & \ddots & \vdots \\ p_{r1} & \cdots & p_{rr} \end{bmatrix}$$

The probability to be in the state i and reach the state j is given by p_{ij} (Equation 14)

$$p_{ij} = P_r\{X_n = j \mid X_{n-1} = i\} \tag{14}$$

Although Equation 14 provides the probability of being in the same state (rii or rjj), it does not provide the state's duration (i.e., persistence). The persistence time or time duration is defined as the time of a sample to remain in the same STMP. Then, to estimate the time duration of the STMPs for each group, we calculated the persistence time defined as D (Equation 15).

$$D(i) = \frac{n_i}{p_i} \times 0.06 \tag{15}$$

where i is the STMP group, ni is the amount of the samples in *i-th* STMP group, and ri is the number of permanence blocks for the *i-th* STMP type. The permanence block is the set of samples consecutive of the same STMP (Figure 21). The constant 0.06 converts the value into milliseconds. In the case of ri=0, we considered $D(i)$=ni.

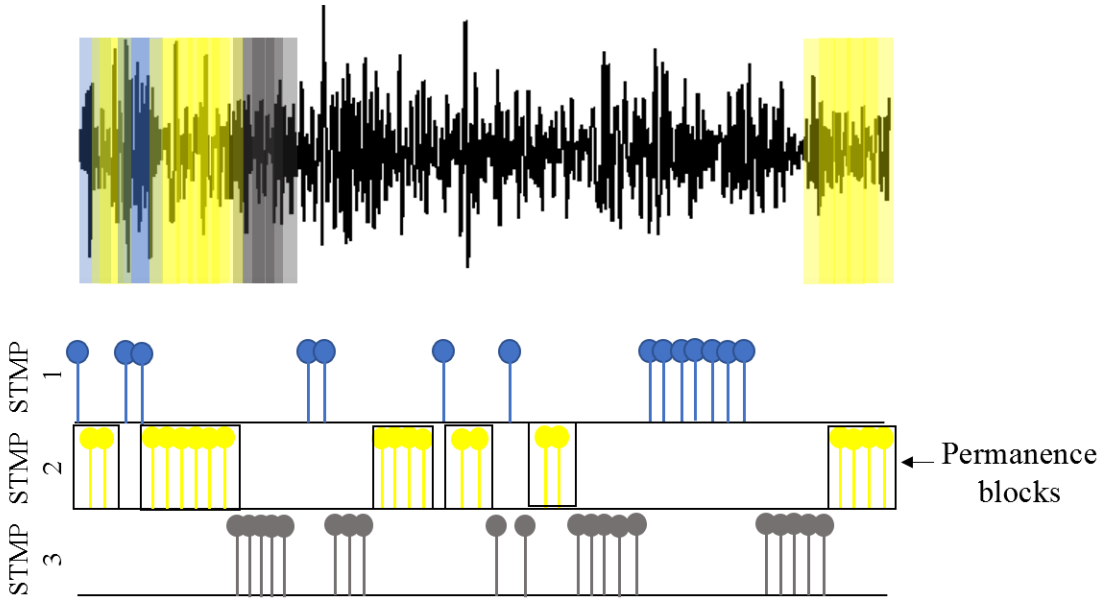

$$D(2) = \frac{n_2}{r_2} \text{ x } 0.06 = \frac{20}{6} \text{ x } 0.06 = 0.2\ ms$$

Figure 21: Calculation of the persistence time (Equation 15) for the STMP 2. Three STMPs (represented by colors blue, yellow, and gray) were identified and distributed along the tremor signal and plotted below according to their appearance order. For STMP 2, the number of samples $n2$ was 20, the number of permanence blocks was 6, and the calculated persistence time was 0.2 ms.

Figure 21 illustrates how persistence time is calculated. We estimated the persistence time for the STMP group identified as 2. Two steps should be followed to calculate duration time in any STMP group. In this case for STMP 2:

- The number of samples in the STMP 2 was n_2=20
- The number of permanence blocks for each transition for the STMP 2 was $r = 6$

Thus, we obtained the persistence time of 0.2 ms for STMP 2 (Figure 21).

5.3.2 STMPs characterization

To characterize each STMP in terms of the extracted features, we calculated the average for all features for each STMP for the HC and PD groups. Since the distribution of the data did not fit a normal distribution (Shapiro–Wilk test, $p < 0.05$), the Wilcoxon test was performed to compare the difference between the groups (HC and PD), with a significance level of 95% ($p < 0.05$).

6. Results

6.1 Explorative cluster analysis

The results from the k-means clustering were obtained from the feature vectors estimated from the data in a lower dimensional space estimated by t-SNE. The gap statistic and a Silhouette plot [97] were employed to estimate the optimal number of clusters (k) (Figure 22). According to both methods, k = 3 allowed for the identification of three clusters, i.e., STMP templates.

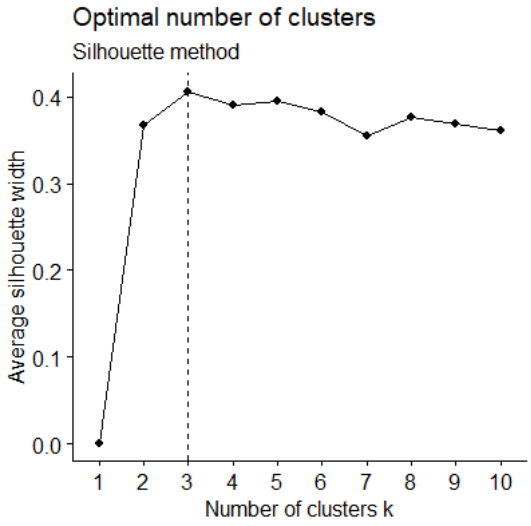

Figure 22: Silhouette plot indicating the optimal number of clusters (k) equals to 3

Furthermore, to confirm the findings above, we tested the differences between pairwise clusters through the Fasano–Franceschini test ($p < 0.05$) (Table 7).

Table 7: differences among pairwise clusters of STMPs given by the Fasano–Franceschini test

Clusters	D-statistic	p-statistic
1 and 2	0.87	< 0.05*
1 and 3	0.97	< 0.05*
2 and 1	0.87	< 0.05*

Significant results for the differences among pairwise clusters are highlighted with "*", for each condition.

The results presented in Table 7 showed that the differences among pairwise clusters were significant. The statistical results supported our decision that three clusters gave us an optimal solution.

6.2 Identification of STMPs

From the analysis of clusters above, we identified three distinct types of STMPs present in the tremor in PD individuals. The distribution of these STMPs according to their similarity and groups (HC or PD) is shown in Figure 23.

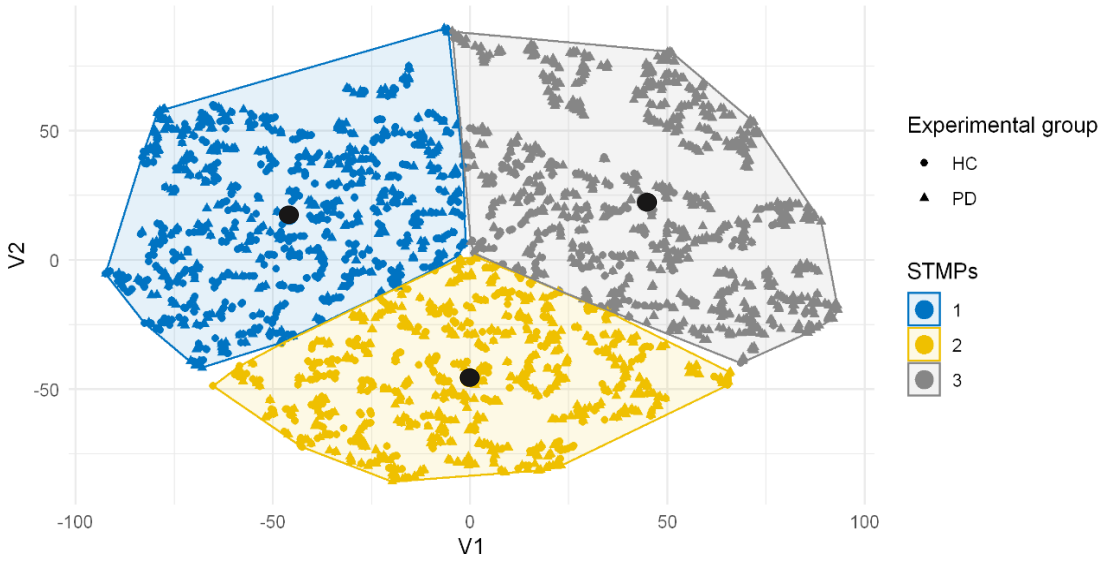

Figure 23: Distribution in three STMPs of all signal segments of both groups (HC and PD). The black circles highlight the cluster centers estimated by k−means. The STMP 1 (blue) has a predominance of individuals from control group. STMP 2 (yellow) has both experimental groups, while in STMP 3 (gray) most STMPs are from individuals with PD.

Figure 23 highlights the difference among STMPs. For STMP 1, most STMPs are from individuals in the control group. For STMP 3, most STMPs are from individuals with PD. For STMP 2, both experimental groups presented STMPs with a similar frequency.

6.3 STMPs assessment

The STMPs were assessed based on their frequency as well as the transition probability underlying their occurrences. Figure 24 shows the frequency of STMPs according to their similarity (i.e., STMP 1, 2, or 3) and experimental groups (HC and PD).

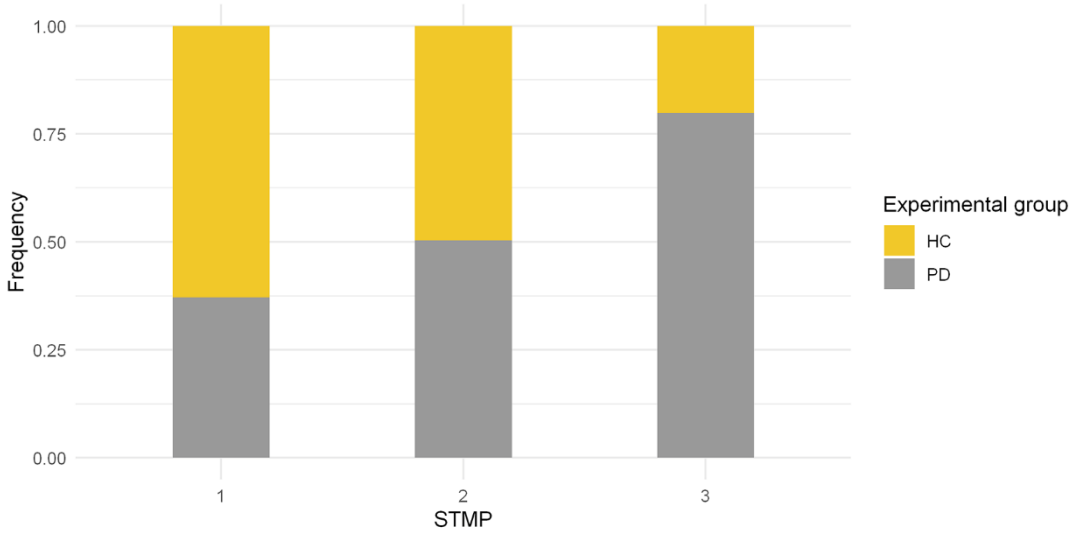

Figure 24: Frequency of STMPs based on each experimental group.

As shown in Figure 24, STMP 1 is more similar to those of the control group. In comparison, approximately 80% of STMP 3 belonged to people with Parkinson's disease. STMP 2 had an equivalence number of STMPs in both experimental groups.

Figure 25 shows the typical STMPs for the HC and PD groups. Although the signals from individuals with PD contained more segments with STMP 3 (Figure 25 - D), those individuals whose tremor was moderate had STMP 1 and 2 (Figure 25 - C), and the time series was similar to that of healthy individuals (Figure 25 - B).

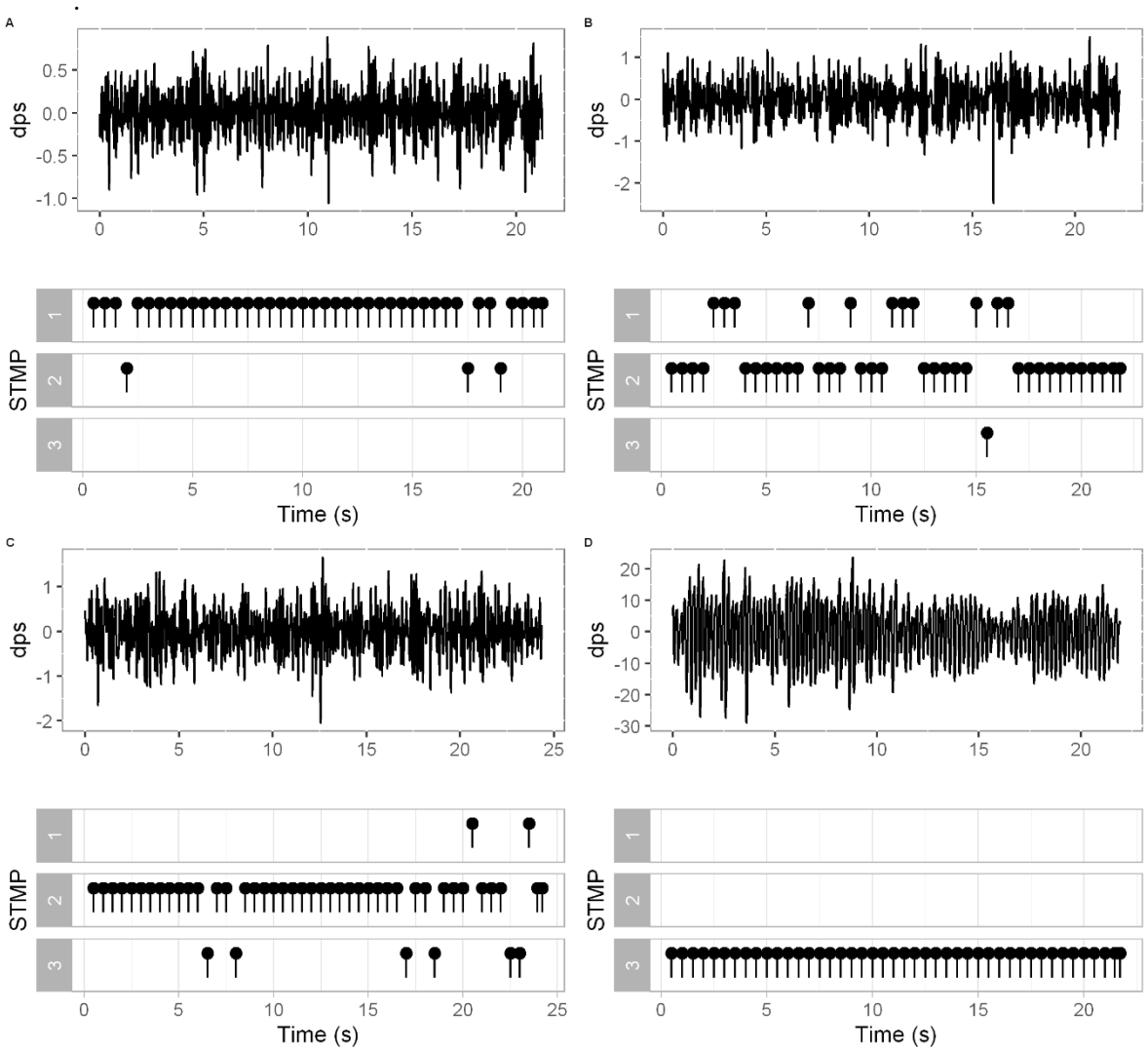

Figure 25: STMPs distributed along the tremor time series obtained from the gyroscope axis X. (A) Tremor signal from a healthy individual with the prevalence of STMP 1. (B) Tremor signal from a healthy individual with STMPs of all types. However, most of them are STMP 1 and 2. (C) Tremor signal from an individual with PD. Most of the STMPs are type 2. (D) Severe tremor signal from an individual with PD with the prevalence of STMPs type 3.

Additionally, we evaluated the dynamics of the STMPs according to the transition probability of their occurrence and the time of permanence in the underlying states related to the distinct STMPs types.

For the assessment of the transition, we adopted the transition probability matrix to calculate the probability of one STMP to transit to another one (Figure 26).

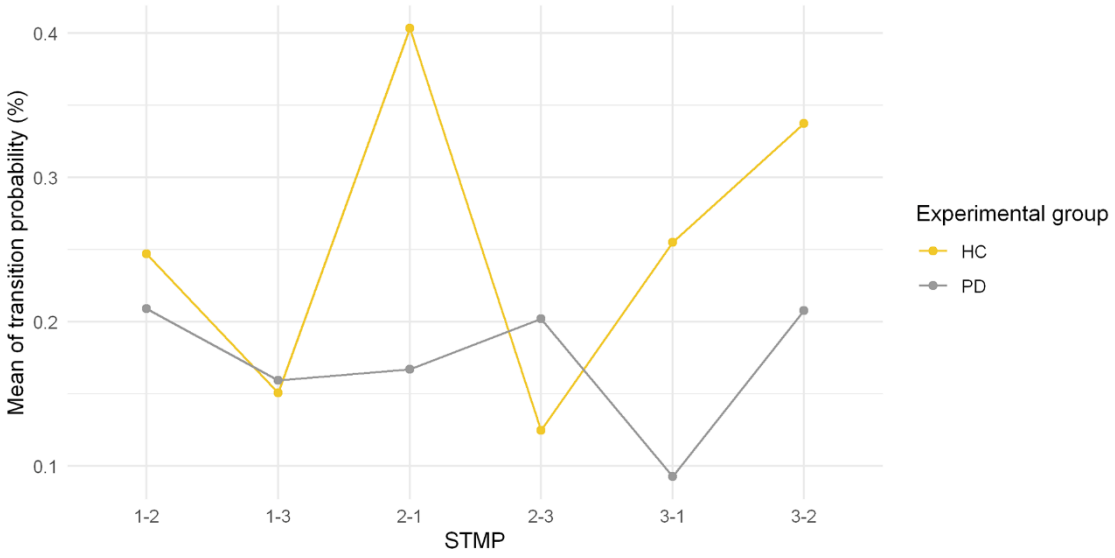

Figure 26: Transition probability between the STMP for each group (HC and PD).

As presented in Figure 26, the HC group presented the highest transition values, especially from the 2 to 1 and 3 to 2 STMP types, whereas the PD group showed the lowest transition values.

The permanence time in each STMP type was calculated according to Equation (3) for each group. Figure 27 illustrates the mean permanence time in ms of each STMP type.

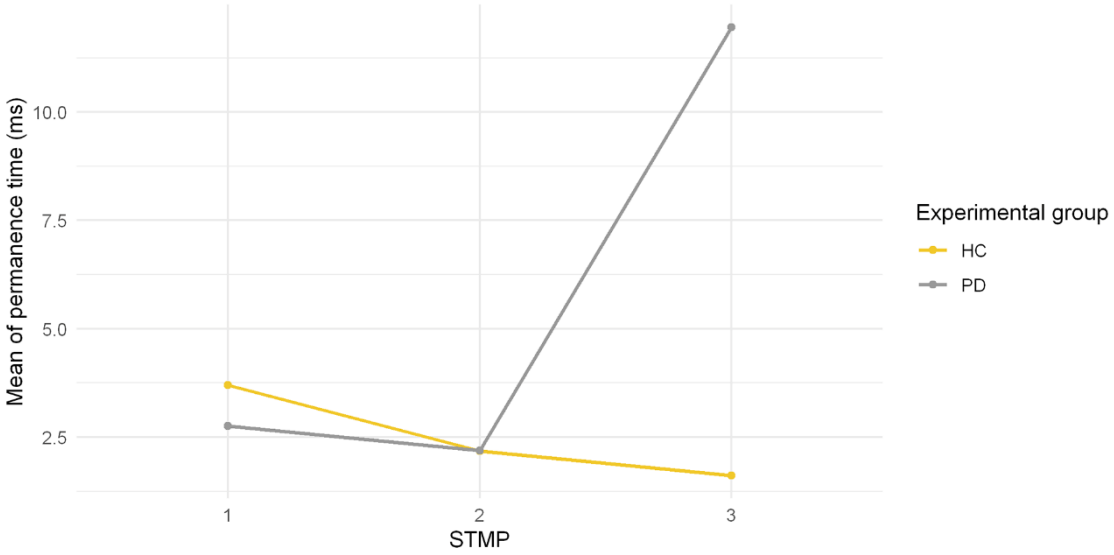

Figure 27: Mean of permanence time in each STMP for groups.

As shown in Figure 27, the PD group presented the highest mean permanence time (up to 10 ms in STMP 3). In contrast, the HC group presented about 3 ms in STMP 1. In STMP 2, both groups presented similar values of the mean permanence time, around 2.45 ms.

6.4 STMPs characterization

The STMPs were characterized in terms of the extracted features. Table 8 shows the average for all the extracted features for both groups for each STMP type. Only CV and COMP were not significantly different ($p > 0.05$) between the HC and PD groups.

Table 8: Mean of the extracted features for each STMP type for both groups

Features	STMP	HC group (mean ± std)	PD group (mean ± std)	p-value
MAV	1	0.27 ± 0.13	4.10 ± 31.81	< 0.05*
	2	0.32 ± 0.13	0.68 ± 1.12	< 0.05*
	3	0.28 ± 0.14	30.59 ± 45.21	< 0.05*
CV	1	82.71 ± 1128.10	861.72 ± 17606.78	3.14×10^{-1}
	2	-3.19 ± 435.55	-53.84 ± 517.96	7.78×10^{-2}
	3	25.26 ± 240.14	14.37 ± 457.44	9.75×10^{-1}
ZRC	1	6.32e-2 ± 6.90×10^{-3}	6.43e-2 ± 1.01×10^{-2}	< 0.05*
	2	5.15e-2 ± 5. 80×10^{-3}	4.95e-2 ± 5.90×10^{-3}	< 0.05*
	3	4.80e-2 ± 8.62×10^{-3}	3.75e-2 ± 1.06×10^{-2}	< 0.05*
SampEn	1	0.52 ± 4.27×10^{-2}	0.51 ± 6.40×10^{-2}	< 0.05*
	2	0.48 ± 5.08×10^{-2}	0.46 ± 5.12×10^{-2}	< 0.05*
	3	0.46 ± 6.74×10^{-2}	0.37 ± 8.80×10^{-2}	< 0.05*
VAR	1	0.14 ± 0.19	1378.22 ± 11695.60	< 0.05*
	2	0.19 ± 0.19	2.62 ± 18.21	< 0.05*
	3	0.16 ± 0.22	4000.02 ± 10009.58	< 0.05*
MOB	1	0.20 ± 1.83×10^{-2}	0.20 ± 2.85×10^{-2}	< 0.05*
	2	0.17 ± 1.4×10^{-2}	0.16 ± 1.55×10^{-2}	< 0.05*
	3	0.16 ± 2.07×10^{-2}	0.13 ± 2.85	< 0.05*
COMP	1	1.42 ± 0.14	1.45 ± 0.17	5.72×10^{-2}
	2	1.39 ± 0.13	1.40 ± 0.13	2.84×10^{-1}
	3	1.77 ± 0.18	1.67 ± 0.31	< 0.05*

Significant results for the differences among the groups for each STMP are highlighted with "*".

7. Discussion

Tremor characterization is critical for developing appropriate individualized treatment and rehabilitation strategies. According to our findings, there are at least three STMPs that are significantly different in tremor signals, and these STMPs can be characterized and evaluated based on amplitude, time of permanence and transition, and complexity. We found that the tremulous motion of the hand provided novel insights into the underlying temporal aspects of tremors that may be used as diagnostic and prognostic biomarkers for tremors.

The exploratory data analysis yielded valuable insights into the characteristics of tremor signals (Figure 8). Through visualization and inspection, we identified the presence of short patterns in the tremor signals (Figure 13), which was further confirmed by employing Empirical Mode Decomposition (EMD). EMD, introduced by E. Rocon and colleagues in 2006, is a nonlinear technique that does not require stationarity or linearity as prerequisites [41]. It is a high-resolution method that serves as an alternative to Fourier-based analysis, which is the standard technique for studying tremor time series. E. Rocon and colleagues applied EMD to evaluate signals collected from 31 patients with different neurological conditions and concluded that the First Intrinsic Mode Function (IMF) is more closely related to tremor [41]. In a similar study, Lee A. et al. assessed tremors in violinists using EMD and found that the third IMF contained more meaningful information about tremor. However, they suggested combining the second and third IMF for tremor analysis [42].

Based on our findings, the divergence regarding which IMF is most related to tremor [41], [42] may be attributed to the type and severity of the tremor. We observed that for mild or moderate tremors, the second and first IMF components are more representative, while for more severe tremors, the third component is a suitable choice. Consequently, we opted to inspect each signal separately to account for these variations (Figure 13).

The experimental protocol and signal pre-processing were based on the study from Andrade et al. [99]. The protocol used a pair of triaxial inertial units positioned on the back of the hand (Figure 5). Due to simplicity and the reported results in a previous study [99], we adopted the same protocol. However, only data from the gyroscope placed on the hand were used for analysis. In addition, to improve the data quality from gyroscope X, linear and nonlinear trends from the signals were removed following the same pre-processing steps described in [99]. As we investigated the short pieces of the signal, it is crucial to guarantee that small motions unrelated to the tremor motion and noise from the device are removed.

The sensor and axis were chosen using a strategy based on the exploratory data analysis and clustering of STMPs (Figure 23). Because the tremor manifests in all directions, we tested other sensors (e.g., an accelerometer and gyroscope) to determine which was best for detecting

STMPs. The sensor performance based on the clustering results from gyroscope axis X (Figure 23) was more relevant for our purposes. Furthermore, in the setting shown in Figure 5, the gyroscope captured hand tremors better, particularly around the X-axis, where a tremor corresponding to small amplitude movements of wrist adduction/abduction (radial–ulnar deviation) and forearm pronation/supination occurs, and such movements are more pronounced than movements around the Y axis, which correspond to movements of wrist flexion/extension.

The main focus of most tremor studies is detecting or comparing the tremor of different groups/conditions and extracting features of the whole signal [42], [61], [100]–[102]. However, to identify underlying patterns in tremor signals, it is necessary to track them since tremors change over time. Thus, all signals were segmented with a 50% overlapping window to explore their dynamics [103]. A window size of 1 second was selected after observing the occurrence of these short patterns in the tremor signal (Figure 13). These Short-Term Movement Patterns (STMPs) typically appear for durations of 1 second or less within the signal. Furthermore, it is important to note that sample entropy is sensitive to the number of samples used for analysis. According to the literature [77], [100], reliable estimates of sample entropy require a minimum of 250 samples.

The set of variables used in this study was based on previous studies [3], [77], [99], and tested on simulated signals (Figure 14-18). While the intention was not to simulate a realistic tremor signal in this study, we varied certain parameters present in tremor signals, such as amplitude, frequency, and shape variations. This step was crucial in order to understand the behavior of the features. For each segment, linear and nonlinear features were extracted (APPENDIX A), as linear and nonlinear features provide complementary information for tremor assessment [104]. Morrison et al. [102] emphasized the importance of assessing the pattern of the tremor signal using nonlinear features. According to the authors, it is not always simple to discriminate different forms of tremor using only standard linear measures such as mean amplitude or the dispersion around a mean as traditionally defined. Table 8 highlights the importance of these feature combinations. It is possible to discriminate the groups using some of the features.

The instantaneous fluctuations present in the signal contain physiologically meaningful patterns across multiple temporal–spatial scales. This study identified three (Figure 23) types of STMPs that were significantly different in the tremor signals (Table 7). T-SNE produced the visualization of STMPs (Figure 23), discriminating the different types of STMPs. Moreover, regarding discrimination among the STMP types, t-SNE was a relevant tool applied before executing the clustering step. Similarly, Oliveira et al. [105] found the highest accuracy in applying t-SNE as an a priori step to the classification. To our knowledge, this is the first study reporting cluster analysis techniques to examine STMPs in tremor signals using inertial sensors.

This approach supported the concept that tremors are heterogeneous since we could identify a sequence of different STMPs in the tremor signal from a PD individual. Figure 24 shows that STMP 1 was present mainly in tremor signals from healthy people, although it was also present in tremors from PD individuals. Furthermore, the number of STMP 2s increased substantially in the PD individuals (Figure 25 - C), and STMP 3 was prevalent in PD individuals with a higher UPDRs score (Figure 25 - D).

Similarly, Dietz et al. [7] described that tremors in PD might be characterized by motor unit discharges. According to the authors, in those periods that the grouped discharges were more regular, the tremor amplitude decreased, and the firing frequency increased. Sometimes in these discharge periods, the tremor may disappear. It means that in a single tremor signal, it is possible to find distinct types of STMPs, as shown in Figure 25 – B and C. In addition, corroborating this result, Agapaki et al. [6] demonstrated the similarities between the characteristics and the activity of MUs in interspike intervals within doublets/triplets of tremors in PD and physiological tremors.

Some signals from healthy people presented STMP 3, although about 80% of the signals from people with PD presented STMP 3. Comparing the results with the UPDRS scores of the PD group, signals containing a large number of STMP 1 were from PD individuals with a more moderate tremor. In contrast, those people from the PD group whose signals presented a large number of STMP 3s had a more severe tremor (Figure 25 - D). Surprisingly, some individuals in the HC group presented an expressive number of STMP 3s in their signals, possibly indicating the presence of a smoother tremor. A possible explanation for this result is that most people from HC are older adults, suggesting that tremors are related to aging, in which there exist segments of STMP 3 [106].

STMP 2 represents tremulous patterns associated with an intermediary state present for both groups in the same proportion. Interestingly, the appearance frequency of STMP2 may be related to tremor severity, as seen in the values of permanence time and transition probability (Figure 26 and Figure 27). STMP 2 is present in the signal of HC individuals all the time (Figure 26); thus, it has a higher mean probability of transition and lower permanence time in a single STMP (Figure 27). In contrast, the signal of PD individuals tends to have a lower transition probability and higher permanence time (Figure 26 and Figure 27). We may consider this higher transition probability from HC as variability, which provides adaptive strategies to maintain the control of tremors. Harbourne and Stergiou [107] emphasized the relevance of variability for maintaining health. They highlight that a lack of variability traps a behavior in a specific state or pattern, as shown in Figure 10 with the PD group. Individuals with PD tended to stay in state 3 related to STMP 3 for almost 30 ms (Figure 27), while healthy individuals stayed in state 1, related to STMP 1, for about 3 ms. Figure 25 - D shows a severe tremor; therefore, the whole signal had

STMP 3. Then, we suggest that permanence time and transition probability in STMPs might be a source of behavioral change.

According to Harbourne and Stergiou [107], nonlinear tools best capture the hidden information in the variability, quantifying the structure of the signal. Sample entropy is a nonlinear tool used for measuring the degree of predictability or the structure of the variability of a time series. The difference among the STMPs of both groups was significant (Table 8, $p < 0.05$). For HC, the sample entropy values were higher than those for the PD group, indicating that the tremor was more regular and more predictable in the PD group. Similar results were found in studies where the tremor variability was around 15–22% lower in PD patients than in healthy controls, and the tremor was more regular in PD [69], [101], [102], [108].

Furthermore, Gil et al. investigated entropy to evaluate hand tremors. They observed a 59.8% decrease in entropy for the resting tremor in PD patients and an increased tremor amplitude for these patients [86]. Similarly, Rissanen et al. [60] concluded that the EMG signals of PD individuals are more regular and contain more recurrent patterns than the EMG signals of healthy individuals. These previous findings supported our findings that the signals of individuals with PD are more regular (with less variability) than healthy individuals.

7.1 Limitations

- The sample size (N = 26) was determined according to the literature. Many studies evaluated tremors with similar samples size and reached significant results [6], [7], [99], [101], [102], [109]. A greater sample size would validate the finding that tremors are heterogeneous, and more samples of each tremor severity may better characterize the signs of tremors.
- Although the selection of a 1-second window size was based on the examination of the extracted IMFs from the signal, employing an automated tool for detecting the start and end of each STMP could provide additional insights into the short patterns present in the tremor signal.
- The present study is the first to evaluate STMPs using inertial sensors. In order to ensure the reliability of the results, it is important to validate them by comparing them with other studies that have also identified short patterns, such as [6].

8. Conclusion and recommendations

8.1 Main contributions of this research

This study described a method to identify and characterize STMPs in tremor signals. We assessed these STMPs from data obtained from a gyroscope placed on the dorsal side of the hand. We identified three STMPs in tremor signals and observed their prevalence depending on the tremor type, i.e., pathological or physiological, and individual condition. Moreover, we characterized these STMPs in terms of amplitude, permanence time, and complexity. The results confirm that tremors in individuals with PD tend to get trapped in a specific state. Therefore, this signal is less complex than the tremor in HC.

In this sense, the methods used in this study can identify relevant landmarks for the follow up with tremor symptoms, assisting professionals in evaluating the tremor severity and the efficacy of a treatment.

8.2 Further studies

Although the present study has demonstrated the presence of short patterns in the tremor signals of healthy individuals and those with Parkinson's disease (PD), these patterns appear to be random. Additionally, the characteristics of these patterns, such as their shape and frequency, may also exhibit randomness. Thus, it will be interesting for further studies to investigate this inherent randomness for the development of models that can predict the dynamic nature of tremors and propose personalized treatment approaches for individuals with PD.

References

[1] M. F. Dirkx and M. Bologna, “The pathophysiology of Parkinson’s disease tremor,” *J. Neurol. Sci.*, vol. 435, p. 120196, Apr. 2022. https://doi.org/10.1016/j.jns.2022.120196

[2] H. Dai, P. Zhang, and T. Lueth, “Quantitative Assessment of Parkinsonian Tremor Based on an Inertial Measurement Unit,” *Sensors*, vol. 15, no. 10, pp. 25055–25071, Sep. 2015. https://doi.org/10.3390/s151025055

[3] L. Yao, P. Brown, and M. Shoaran, “Improved detection of Parkinsonian resting tremor with feature engineering and Kalman filtering.,” *Clin. Neurophysiol. Off. J. Int. Fed. Clin. Neurophysiol.*, vol. 131, no. 1, pp. 274–284, Jan. 2020. https://doi.org/10.1016/j.clinph.2019.09.021

[4] N. Shawen *et al.*, “Role of data measurement characteristics in the accurate detection of Parkinson’s disease symptoms using wearable sensors.,” *J. Neuroeng. Rehabil.*, vol. 17, no. 1, p. 52, Apr. 2020. https://doi.org/10.1186/s12984-020-00684-4

[5] L. Yao, P. Brown, and M. Shoaran, “Resting Tremor Detection in Parkinson’s Disease with Machine Learning and Kalman Filtering.,” *IEEE Biomed. Circuits Syst. Conf. Healthc. Technol. [proceedings]. IEEE Biomed. Circuits Syst. Conf.*, vol. 2018, Jun. 2019. https://doi.org/10.1109/BIOCAS.2018.8584721

[6] O. M. Agapaki, C. N. Christakos, and D. Anastasopoulos, “Characteristics of Rest and Postural Tremors in Parkinson’s Disease: An Analysis of Motor Unit Firing Synchrony and Patterns.,” *Front. Hum. Neurosci.*, vol. 12, p. 179, 2018. https://doi.org/10.3389/fnhum.2018.00179

[7] V. Dietz, W. Hillesheimer, and H.-J. Freund, “Correlation between tremor, voluntary contraction, and firing pattern of motor units in Parkinson’s disease,” *J. Neurol. Neurosurg. Psychiatry*, vol. 37, no. 8, pp. 927–937, Aug. 1974. https://doi.org/10.1136/jnnp.37.8.927

[8] J. F. Leslie and C. Rudy, *Movement Disorders: Tremor*. 1984.

[9] I. Rektorova, M. Mikl, J. Barrett, R. Marecek, I. Rektor, and T. Paus, “Functional neuroanatomy of vocalization in patients with Parkinson’s disease.,” *J. Neurol. Sci.*, vol. 313, no. 1–2, pp. 7–12, Feb. 2012. https://doi.org/10.1016/j.jns.2011.10.020

[10] V. L. Feigin *et al.*, “Global, regional, and national burden of neurological disorders, 1990–2016: a systematic analysis for the Global Burden of Disease Study 2016,” *Lancet Neurol.*, vol. 18, no. 5, pp. 459–480, May 2019.

[11] H. Ehringer and O. Hornykiewicz, “Verteilung Von Noradrenalin Und Dopamin (3-Hydroxytyramin) Im Gehirn Des Menschen Und Ihr Verhalten Bei Erkrankungen Des Extrapyramidalen Systems,” *Klin. Wochenschr.*, vol. 38, no. 24, pp. 1236–1239, Dec. 1960. https://doi.org/10.1007/BF01485901

[12] W. J. Weiner, “There Is No Parkinson Disease,” *Arch. Neurol.*, vol. 65, no. 6, Jun. 2008. https://doi.org/10.1001/archneur.65.6.705

[13] S. L. Farrow, A. A. Cooper, and J. M. O’Sullivan, “Redefining the hypotheses driving Parkinson’s diseases research,” *npj Park. Dis.*, vol. 8, no. 1, p. 45, Dec. 2022. https://doi.org/10.1038/s41531-022-00307-w

[14] X. Zheng *et al.*, “Gait and balance in Parkinson’s disease subtypes: objective measures and classification considerations,” *Parkinsonism Relat. Disord.*, vol. 9, no. 1, pp. 1–7, Jun. 2018.

[15] W. R. Gibb and A. J. Lees, “The relevance of the Lewy body to the pathogenesis of idiopathic Parkinson’s disease.,” *J. Neurol. Neurosurg. Psychiatry*, vol. 51, no. 6, pp. 745–752, Jun. 1988. https://doi.org/10.1136/jnnp.51.6.745

[16] J. Jankovic, “Parkinson ’ s disease : clinical features and diagnosis,” *Neurol Neurosurg Psychiatry*, no. 1957, pp. 368–376, 2008. https://doi.org/10.1136/jnnp.2007.131045

[17] E. Tolosa, G. Wenning, and W. Poewe, “The diagnosis of Parkinson’s disease,” *Lancet Neurol.*, vol. 5, no. 1, pp. 75–86, Jan. 2006. https://doi.org/10.1016/S1474-4422(05)70285-4

[18] D. J. Gelb, E. Oliver, and S. Gilman, “Diagnostic Criteria for Parkinson Disease,” *Arch. Neurol.*, vol. 56, no. 1, p. 33, Jan. 1999. https://doi.org/10.1001/archneur.56.1.33

[19] C. G. Goetz *et al.*, “Movement Disorder Society-Sponsored Revision of the Unified Parkinson ’ s Disease Rating Scale (MDS-UPDRS): Scale Presentation and Clinimetric Testing Results,” *Mov. Disordes*, vol. 23, no. 15, pp. 2129–2170, 2008. https://doi.org/10.1002/mds.22340

[20] J. M. Beitz, “Parkinson’s disease: a review.,” *Front. Biosci. (Schol. Ed).*, vol. 6, pp. 65–74, Jan. 2014. https://doi.org/10.2741/S415

[21] J. J. Ferreira *et al.*, “Summary of the recommendations of the EFNS/MDS-ES review on therapeutic management of Parkinson’s disease,” *Eur. J. Neurol.*, vol. 20, no. 1, pp. 5–15, Jan. 2013. https://doi.org/10.1111/j.1468-1331.2012.03866.x

[22] J. M. Miyasaki, W. Martin, O. Suchowersky, W. J. Weiner, and A. E. Lang, “Practice

parameter: Initiation of treatment for Parkinson's disease: An evidence-based review: Report of the Quality Standards Subcommittee of the American Academy of Neurology," *Neurology*, vol. 58, no. 1, pp. 11–17, Jan. 2002. https://doi.org/10.1212/WNL.58.1.11

[23] K. Frei and D. D. Truong, "Medications used to treat tremors," *J. Neurol. Sci.*, vol. 435, p. 120194, Apr. 2022. https://doi.org/10.1016/j.jns.2022.120194

[24] P. S. Fishman, "Paradoxical aspects of parkinsonian tremor," *Mov. Disord.*, vol. 23, no. 2, pp. 168–173, Jan. 2008. https://doi.org/10.1002/mds.21736

[25] H. Zach, M. F. Dirkx, D. Roth, J. W. Pasman, B. R. Bloem, and R. C. Helmich, "Dopamine-responsive and dopamine-resistant resting tremor in Parkinson disease," *Neurology*, vol. 95, no. 11, pp. e1461–e1470, Sep. 2020. https://doi.org/10.1212/WNL.0000000000010316

[26] J. H. McAuley, "Physiological and pathological tremors and rhythmic central motor control," *Brain*, vol. 123, no. 8, pp. 1545–1567, Aug. 2000. https://doi.org/10.1093/brain/123.8.1545

[27] V. Horsley and E. A. Schäfer, "Experiments on the character of the Muscular Contractions which are evoked by Excitation of the various parts of the Motor Tract," *J. Physiol.*, vol. 7, no. 2, pp. 96–110, Apr. 1886. https://doi.org/10.1113/jphysiol.1886.sp000209

[28] S. M. Rissanen *et al.*, "Analysis of EMG and Acceleration Signals for Quantifying the Effects of Deep Brain Stimulation in Parkinson's Disease," *IEEE Trans. Biomed. Eng.*, vol. 58, no. 9, pp. 2545–2553, 2011. https://doi.org/10.1109/TBME.2011.2159380

[29] R. C. Helmich, M. Hallett, G. Deuschl, I. Toni, and B. R. Bloem, "Cerebral causes and consequences of parkinsonian resting tremor: a tale of two circuits?," *Brain*, vol. 135, no. 11, pp. 3206–3226, Nov. 2012. https://doi.org/10.1093/brain/aws023

[30] G. Leodori *et al.*, "Re-emergent Tremor in Parkinson's Disease: The Role of the Motor Cortex," *Mov. Disord.*, vol. 35, no. 6, pp. 1002–1011, Jun. 2020. https://doi.org/10.1002/mds.28022

[31] N. A. Habib-ur-Rehman, "Diagnosis and Management of Tremor," *Arch. Intern. Med.*, vol. 160, no. 16, p. 2438, Sep. 2000. https://doi.org/10.1001/archinte.160.16.2438

[32] L. E. Heusinkveld, M. L. Hacker, M. Turchan, T. L. Davis, and D. Charles, "Impact of Tremor on Patients With Early Stage Parkinson's Disease," *Front. Neurol.*, vol. 9, Aug. 2018. https://doi.org/10.3389/fneur.2018.00628

[33] L. A. Uebelacker, G. Epstein-Lubow, T. Lewis, M. K. Broughton, and J. H. Friedman, "A

Survey of Parkinson's Disease Patients: Most Bothersome Symptoms and Coping Preferences," *J. Parkinsons. Dis.*, vol. 4, no. 4, pp. 717–723, 2014. https://doi.org/10.3233/JPD-140446

[34] G. G. Grimaldi and M. Manto, "Tremor: From Pathogenesis to Treatment," *Synth. Lect. Biomed. Eng.*, vol. 3, no. 1, pp. 1–212, Jan. 2008. https://doi.org/10.2200/S00129ED1V01Y200807BME020

[35] G. Deuschl, F. Papengut, and H. Hellriegel, "The phenomenology of Parkinsonian tremor," *Parkinsonism Relat. Disord.*, vol. 18, pp. S87–S89, Jan. 2012. https://doi.org/10.1016/S1353-8020(11)70028-1

[36] K. P. Bhatia *et al.*, "Consensus Statement on the classification of tremors. from the task force on tremor of the International Parkinson and Movement Disorder Society," *Mov. Disord.*, vol. 33, no. 1, pp. 75–87, Jan. 2018.

[37] T. A. Saifee, "Tremor," *Br. Med. Bull.*, vol. 130, no. 1, pp. 51–63, Jun. 2019. https://doi.org/10.1093/bmb/ldz017

[38] N. Ishii, Y. Mochizuki, K. Shiomi, M. Nakazato, and H. Mochizuki, "Spiral drawing: Quantitative analysis and artificial-intelligence-based diagnosis using a smartphone.," *J. Neurol. Sci.*, vol. 411, p. 116723, Apr. 2020. https://doi.org/10.1016/j.jns.2020.116723

[39] C. M. Laine and F. J. Valero-Cuevas, "Parkinson's Disease Exhibits Amplified Intermuscular Coherence During Dynamic Voluntary Action.," *Front. Neurol.*, vol. 11, p. 204, 2020. https://doi.org/10.3389/fneur.2020.00204

[40] W. Huo *et al.*, "A Heterogeneous Sensing Suite for Multisymptom Quantification of Parkinson's Disease.," *IEEE Trans. neural Syst. Rehabil. Eng. a Publ. IEEE Eng. Med. Biol. Soc.*, Apr. 2020. https://doi.org/10.1109/TNSRE.2020.2978197

[41] E. R. de Lima, A. O. Andrade, J. L. Pons, P. Kyberd, and S. J. Nasuto, "Empirical mode decomposition: a novel technique for the study of tremor time series.," *Med. Biol. Eng. Comput.*, vol. 44, no. 7, pp. 569–582, Jul. 2006. https://doi.org/10.1007/s11517-006-0065-x

[42] A. Lee and E. Altenmuller, "Detecting position dependent tremor with the Empirical mode decomposition.," *J. Clin. Mov. Disord.*, vol. 2, p. 3, 2015. https://doi.org/10.1186/s40734-014-0014-z

[43] S. A. Shah, G. Tinkhauser, C. C. Chen, S. Little, and P. Brown, "Parkinsonian Tremor Detection from Subthalamic Nucleus Local Field Potentials for Closed-Loop Deep Brain Stimulation," in *2018 40th Annual International Conference of the IEEE Engineering in*

Medicine and Biology Society (EMBC), 2018, pp. 2320–2324. https://doi.org/10.1109/EMBC.2018.8512741

[44] M. D. Hssayeni, M. A. Burack, J. Jimenez-Shahed, and B. Ghoraani, "Assessment of response to medication in individuals with Parkinson's disease," *Med. Eng. Phys.*, vol. 67, pp. 33–43, May 2019. https://doi.org/10.1016/j.medengphy.2019.03.002

[45] B. Houston, Z. Blumenfeld, E. Quinn, H. Bronte-Stewart, and H. Chizeck, "Long-term detection of Parkinsonian tremor activity from subthalamic nucleus local field potentials.," *Conf. Proc. ... Annu. Int. Conf. IEEE Eng. Med. Biol. Soc. IEEE Eng. Med. Biol. Soc. Annu. Conf.*, vol. 2015, pp. 3427–3431, 2015. https://doi.org/10.1109/EMBC.2015.7319129

[46] H. M. Teager and S. M. Teager, "Evidence for Nonlinear Sound Production Mechanisms in the Vocal Tract," in *Speech Production and Speech Modelling*, Dordrecht: Springer Netherlands, 1990, pp. 241–261. https://doi.org/10.1007/978-94-009-2037-8_10

[47] M. A. Hanson, H. C. Powell, R. C. Frysinger, D. S. Huss, W. J. Elias, and J. Lach, "Teager energy assessment of tremor severity in clinical application of wearable inertial sensors," in *2007 IEEE/NIH Life Science Systems and Applications Workshop*, 2007, pp. 136–139. https://doi.org/10.1109/LSSA.2007.4400903

[48] S. M. Rissanen *et al.*, "Analysis of dynamic EMG and acceleration measurements in Parkinson's disease," in *2008 30th Annual International Conference of the IEEE Engineering in Medicine and Biology Society*, 2008, pp. 5053–5056. https://doi.org/10.1109/IEMBS.2008.4650349

[49] G. Di Lazzaro *et al.*, "Technology-Based Objective Measures Detect Subclinical Axial Signs in Untreated, de novo Parkinson's Disease.," *J. Parkinsons. Dis.*, vol. 10, no. 1, pp. 113–122, 2020. https://doi.org/10.3233/JPD-191758

[50] N. Ferenčík, M. Jaščur, M. Bundzel, and F. Cavallo, "The Rehapiano-Detecting, Measuring, and Analyzing Action Tremor Using Strain Gauges.," *Sensors (Basel).*, vol. 20, no. 3, Jan. 2020. https://doi.org/10.3390/s20030663

[51] C. Camara, N. P. Subramaniyam, K. Warwick, L. Parkkonen, T. Aziz, and E. Pereda, "Non-Linear Dynamical Analysis of Resting Tremor for Demand-Driven Deep Brain Stimulation.," *Sensors (Basel).*, vol. 19, no. 11, May 2019. https://doi.org/10.3390/s19112507

[52] C. D. Rios-Urrego, J. C. Vasquez-Correa, J. F. Vargas-Bonilla, E. Noth, F. Lopera, and J. R. Orozco-Arroyave, "Analysis and evaluation of handwriting in patients with Parkinson's

disease using kinematic, geometrical, and non-linear features.," *Comput. Methods Programs Biomed.*, vol. 173, pp. 43–52, May 2019. https://doi.org/10.1016/j.cmpb.2019.03.005

[53] P. Y. Chan *et al.*, "Biomechanical System Versus Observational Rating Scale for Parkinson's Disease Tremor Assessment," *Sci. Rep.*, vol. 9, no. 1, p. 8117, Dec. 2019. https://doi.org/10.1038/s41598-019-44142-1

[54] D. Haubenberger *et al.*, "Transducer-based evaluation of tremor.," *Mov. Disord.*, vol. 31, no. 9, pp. 1327–1336, Sep. 2016. https://doi.org/10.1002/mds.26671

[55] G. Deuschl, J. Raethjen, R. Baron, M. Lindemann, H. Wilms, and P. Krack, "The pathophysiology of parkinsonian tremor: a review," *J. Neurol.*, vol. 247, no. S5, pp. V33–V48, Oct. 2000. https://doi.org/10.1007/PL00007781

[56] F. Stocchi, P. Jenner, and J. A. Obeso, "When do levodopa motor fluctuations first appear in Parkinson's disease?," *Eur. Neurol.*, vol. 63, no. 5, pp. 257–266, 2010. https://doi.org/10.1159/000300647

[57] M. K. Erb *et al.*, "mHealth and wearable technology should replace motor diaries to track motor fluctuations in Parkinson's disease.," *NPJ Digit. Med.*, vol. 3, p. 6, 2020. https://doi.org/10.1038/s41746-019-0214-x

[58] J. E. Thorp, P. G. Adamczyk, H.-L. Ploeg, and K. A. Pickett, "Monitoring Motor Symptoms During Activities of Daily Living in Individuals With Parkinson's Disease.," *Front. Neurol.*, vol. 9, p. 1036, 2018. https://doi.org/10.3389/fneur.2018.01036

[59] R. Erro, A. Fasano, P. Barone, and K. P. Bhatia, "Milestones in Tremor Research: 10 Years Later," *Mov. Disord. Clin. Pract.*, vol. 9, no. 4, pp. 429–435, May 2022. https://doi.org/10.1002/mdc3.13418

[60] S. M. Rissanen *et al.*, "Analysis of dynamic EMG and acceleration measurements in Parkinson's disease," in *2008 30th Annual International Conference of the IEEE Engineering in Medicine and Biology Society*, 2008, pp. 5053–5056. https://doi.org/10.1109/IEMBS.2008.4650349

[61] A. de Oliveira Andrade *et al.*, "Task-Specific Tremor Quantification in a Clinical Setting for Parkinson's Disease," *J. Med. Biol. Eng.*, vol. 40, no. 6, pp. 821–850, Dec. 2020. https://doi.org/10.1007/s40846-020-00576-x

[62] A. G. Rabelo *et al.*, "Objective Assessment of Bradykinesia Estimated from the Wrist Extension in Older Adults and Patients with Parkinson's Disease.," *Ann. Biomed. Eng.*, vol. 45, no. 11, pp. 2614–2625, Nov. 2017. https://doi.org/10.1007/s10439-017-1908-3

[63] A. R. P. Machado *et al.*, "Feature visualization and classification for the discrimination between individuals with Parkinson's disease under levodopa and DBS treatments," *Biomed. Eng. Online*, vol. 15, no. 1, p. 169, Dec. 2016. https://doi.org/10.1186/s12938-016-0290-y

[64] M. Komorowski, D. C. Marshall, J. D. Salciccioli, and Y. Crutain, "Exploratory Data Analysis," in *Secondary Analysis of Electronic Health Records*, Cham: Springer International Publishing, 2016, pp. 185–203. https://doi.org/10.1007/978-3-319-43742-2_15

[65] H. Patel, S. Guttula, R. S. Mittal, N. Manwani, L. Berti-Equille, and A. Manatkar, "Advances in Exploratory Data Analysis, Visualisation and Quality for Data Centric AI Systems," in *Proceedings of the 28th ACM SIGKDD Conference on Knowledge Discovery and Data Mining*, 2022, pp. 4814–4815. https://doi.org/10.1145/3534678.3542604

[66] A. J. Barbour and R. L. Parker, "psd: Adaptive, sine multitaper power spectral density estimation for R," *Comput. Geosci.*, vol. 63, pp. 1–8, Feb. 2014. https://doi.org/10.1016/j.cageo.2013.09.015

[67] R Core Team, R. C. Team, R Core Team (2016), and R. C. Team, "R: A language and environment for statistical computing." R Foundation for Statistical Computing, Vienna, Austria, 2017.

[68] J. Jankovic, "Parkinson's disease: clinical features and diagnosis," *J. Neurol. Neurosurg. Psychiatry*, vol. 79, no. 4, pp. 368–376, Apr. 2008. https://doi.org/10.1136/jnnp.2007.131045

[69] A. Y. Meigal *et al.*, "Linear and nonlinear tremor acceleration characteristics in patients with Parkinson's disease," *Physiol. Meas.*, vol. 33, no. 3, pp. 395–412, Mar. 2012. https://doi.org/10.1088/0967-3334/33/3/395

[70] E. Rocon, J. L. L. Pons, A. O. O. Andrade, and S. J. J. Nasuto, "Application of EMD as a novel technique for the study of tremor time series," in *2006 International Conference of the IEEE Engineering in Medicine and Biology Society*, 2006, vol. Suppl, pp. 6533–6536. https://doi.org/10.1109/IEMBS.2006.260871

[71] A. O. Andrade, "Decomposition and Analysis of Electromyographic Signals," THE UNIVERSITY OF READING, 2005.

[72] A. A. Lee, E. Altenmüller, and E. Altenmuller, "Detecting position dependent tremor with the Empirical mode decomposition," *J. Clin. Mov. Disord.*, vol. 2, no. 1, p. 3, Dec. 2015. https://doi.org/10.1186/s40734-014-0014-z

[73] A. O. Andrade, P. J. Kyberd, and S. D. Taffler, "A novel spectral representation of electromyographic signals," in *Proceedings of the 25th Annual International Conference of the IEEE Engineering in Medicine and Biology Society (IEEE Cat. No.03CH37439)*, pp. 2598–2601.

[74] D. Kim and H.-S. Oh, "EMD: A Package for Empirical Mode Decomposition and Hilbert Spectrum," *R J.*, vol. 1, no. 1, p. 40, 2009. https://doi.org/10.32614/RJ-2009-002

[75] A. Rabelo *et al.*, "Low Amplitude Hand Rest Tremor Assessment in Parkinson's Disease Based on Linear and Nonlinear Methods," 2022, pp. 301–306. https://doi.org/10.1007/978-3-030-70601-2_46

[76] C. G. Goetz *et al.*, "Movement Disorder Society-sponsored revision of the Unified Parkinson's Disease Rating Scale (MDS-UPDRS): Process, format, and clinimetric testing plan," *Mov. Disord.*, vol. 22, no. 1, pp. 41–47, Jan. 2007. https://doi.org/10.1002/mds.21198

[77] A. Delgado-Bonal and A. Marshak, "Approximate Entropy and Sample Entropy: A Comprehensive Tutorial," *Entropy*, vol. 21, no. 6, p. 541, May 2019. https://doi.org/10.3390/e21060541

[78] L. C. V. Ferreira, A. G. Rabelo, M. F. Vieira, A. A. Pereira, and A. O. Andrade, "Gait variability and symmetry assessment with inertial sensors for quantitative discrimination of Trendelenburg sign in total hip arthroplasty patients: A pilot study based on convenience sampling," *Res. Biomed. Eng.*, vol. 34, no. 1, 2018. https://doi.org/10.1590/2446-4740.07017

[79] S. Abbaspour, M. Lindén, H. Gholamhosseini, A. Naber, and M. Ortiz-Catalan, "Evaluation of surface EMG-based recognition algorithms for decoding hand movements," *Med. Biol. Eng. Comput.*, vol. 58, no. 1, pp. 83–100, Jan. 2020. https://doi.org/10.1007/s11517-019-02073-z

[80] Z. Arief, I. A. Sulistijono, and R. A. Ardiansyah, "Comparison of five time series EMG features extractions using Myo Armband," in *2015 International Electronics Symposium (IES)*, 2015, pp. 11–14. https://doi.org/10.1109/ELECSYM.2015.7380805

[81] T. T. Henderson, J. R. Thorstensen, S. Morrison, M. G. Tucker, and J. J. Kavanagh, "Physiological tremor is suppressed and force steadiness is enhanced with increased availability of serotonin regardless of muscle fatigue," *J. Neurophysiol.*, vol. 127, no. 1, pp. 27–37, Jan. 2022. https://doi.org/10.1152/jn.00403.2021

[82] C. Ni *et al.*, "Tracking motion kinematics and tremor with intrinsic oscillatory property of instrumental mechanics," *Bioeng. Transl. Med.*, vol. 8, no. 2, Mar. 2023.

https://doi.org/10.1002/btm2.10432

[83] G. F. Inbar, O. Paiss, J. Allin, and H. Kranz, "Monitoring surface EMG spectral changes by the zero crossing rate," *Med. Biol. Eng. Comput.*, vol. 24, no. 1, pp. 10–18, Jan. 1986. https://doi.org/10.1007/BF02441600

[84] J. M. Yentes, N. Hunt, K. K. Schmid, J. P. Kaipust, D. McGrath, and N. Stergiou, "The Appropriate Use of Approximate Entropy and Sample Entropy with Short Data Sets," *Ann. Biomed. Eng.*, vol. 41, no. 2, pp. 349–365, Feb. 2013. https://doi.org/10.1007/s10439-012-0668-3

[85] D. Abásolo, R. Hornero, P. Espino, D. Álvarez, and J. Poza, "Entropy analysis of the EEG background activity in Alzheimer's disease patients," *Physiol. Meas.*, vol. 27, no. 3, pp. 241–253, Mar. 2006. https://doi.org/10.1088/0967-3334/27/3/003

[86] L. M. Gil, T. P. Nunes, F. H. S. Silva, A. C. D. Faria, and P. L. Melo, "Analysis of human tremor in patients with Parkinson disease using entropy measures of signal complexity.," *Conf. Proc. Annu. Int. Conf. IEEE Eng. Med. Biol. Soc. IEEE Eng. Med. Biol. Soc. Annu. Conf.*, vol. 2010, pp. 2786–2789, 2010. https://doi.org/10.1109/IEMBS.2010.5626365

[87] D. E. Lake, J. S. Richman, M. P. Griffin, and J. R. Moorman, "Sample entropy analysis of neonatal heart rate variability," *Am. J. Physiol. Integr. Comp. Physiol.*, vol. 283, no. 3, pp. R789–R797, Sep. 2002. https://doi.org/10.1152/ajpregu.00069.2002

[88] B. Hjorth, "EEG analysis based on time domain properties," *Electroencephalogr. Clin. Neurophysiol.*, vol. 29, no. 3, pp. 306–310, Sep. 1970. https://doi.org/10.1016/0013-4694(70)90143-4

[89] M. Mouzé-Amady and F. Horwat, "Evaluation of Hjorth parameters in forearm surface EMG analysis during an occupational repetitive task," *Electroencephalogr. Clin. Neurophysiol. Mot. Control*, vol. 101, no. 2, pp. 181–183, Apr. 1996. https://doi.org/10.1016/0924-980X(96)00316-5

[90] V. Bolón-Canedo, N. Sánchez-Maroño, and A. Alonso-Betanzos, "A review of feature selection methods on synthetic data," *Knowl. Inf. Syst.*, vol. 34, no. 3, pp. 483–519, Mar. 2013. https://doi.org/10.1007/s10115-012-0487-8

[91] V. Blundell, T. Clarke, and D. Williams, "Synthetic signals for signal processing," in *Sensor Signal Processing for Defence (SSPD 2010)*, 2010, pp. 10–10. https://doi.org/10.1049/ic.2010.0229

[92] R. S. A. Araújo, J. C. Tironi, W. D. Parreira, R. C. Borges, J. F. De Paz Santana, and V. R. Q. Leithardt, "Analysis of Adaptive Algorithms Based on Least Mean Square Applied

to Hand Tremor Suppression Control," *Appl. Sci.*, vol. 13, no. 5, p. 3199, Mar. 2023. https://doi.org/10.3390/app13053199

[93] R. McAulay and T. Quatieri, "Speech analysis/Synthesis based on a sinusoidal representation," *IEEE Trans. Acoust.*, vol. 34, no. 4, pp. 744–754, Aug. 1986. https://doi.org/10.1109/TASSP.1986.1164910

[94] A. Ben Rhouma and S. Ben Jebara, "Features based on quasi-sinudoidal modeling for tremor detection in Parkinsonian voice," in *2014 1st International Conference on Advanced Technologies for Signal and Image Processing (ATSIP)*, 2014, pp. 434–439. https://doi.org/10.1109/ATSIP.2014.6834651

[95] L. van der Maaten and G. Hinton, "Visualizing Data using t-SNE," *J. Mach. Learn. Res.*, vol. 9, pp. 2579–2605, 2008.

[96] R. Tibshirani, G. Walther, and T. Hastie, "Estimating the number of clusters in a data set via the gap statistic," *J. R. Stat. Soc. Ser. B (Statistical Methodol.*, vol. 63, no. 2, pp. 411–423, 2001. https://doi.org/10.1111/1467-9868.00293

[97] M. Shutaywi and N. N. Kachouie, "Silhouette Analysis for Performance Evaluation in Machine Learning with Applications to Clustering," *Entropy*, vol. 23, no. 6, p. 759, Jun. 2021. https://doi.org/10.3390/e23060759

[98] G. Fasano and A. Franceschini, "A multidimensional version of the Kolmogorov–Smirnov test," *Mon. Not. R. Astron. Soc.*, vol. 225, no. 1, pp. 155–170, Mar. 1987. https://doi.org/10.1093/mnras/225.1.155

[99] A. de Oliveira Andrade *et al.*, "Task-Specific Tremor Quantification in a Clinical Setting for Parkinson's Disease," *J. Med. Biol. Eng.*, 2020. https://doi.org/10.1007/s40846-020-00576-x

[100] D. Su *et al.*, "Different effects of essential tremor and Parkinsonian tremor on multiscale dynamics of hand tremor," *Clin. Neurophysiol.*, vol. 132, no. 9, pp. 2282–2289, Sep. 2021. https://doi.org/10.1016/j.clinph.2021.04.017

[101] D. Lukšys, G. Jonaitis, and J. Griškevičius, "Quantitative Analysis of Parkinsonian Tremor in a Clinical Setting Using Inertial Measurement Units," *Parkinsons. Dis.*, vol. 2018, pp. 1–7, Jun. 2018. https://doi.org/10.1155/2018/1683831

[102] S. Morrison, N. Cortes, K. M. Newell, P. A. Silburn, and G. Kerr, "Variability, regularity and coupling measures distinguish PD tremor from voluntary 5Hz tremor," *Neurosci. Lett.*, vol. 534, pp. 69–74, Feb. 2013. https://doi.org/10.1016/j.neulet.2012.11.040

[103] A. Dehghani, O. Sarbishei, T. Glatard, and E. Shihab, "A Quantitative Comparison of Overlapping and Non-Overlapping Sliding Windows for Human Activity Recognition Using Inertial Sensors," *Sensors*, vol. 19, no. 22, p. 5026, Nov. 2019. https://doi.org/10.3390/s19225026

[104] M. Bange, S. Groppa, and M. Muthuraman, "Nonlinear irregularities in Parkinson's disease tremor and essential tremor," *Clin. Neurophysiol.*, vol. 132, no. 9, pp. 2255–2256, Sep. 2021. https://doi.org/10.1016/j.clinph.2021.06.002

[105] F. H. M. Oliveira, A. R. P. Machado, and A. O. Andrade, "On the Use of t -Distributed Stochastic Neighbor Embedding for Data Visualization and Classification of Individuals with Parkinson's Disease," *Comput. Math. Methods Med.*, vol. 2018, pp. 1–17, Nov. 2018. https://doi.org/10.1155/2018/8019232

[106] G. Deuschl, I. Petersen, D. Lorenz, and K. Christensen, "Tremor in the elderly: Essential and aging-related tremor," *Mov. Disord.*, vol. 30, no. 10, pp. 1327–1334, Sep. 2015. https://doi.org/10.1002/mds.26265

[107] R. T. Harbourne and N. Stergiou, "Movement Variability and the Use of Nonlinear Tools: Principles to Guide Physical Therapist Practice," *Phys. Ther.*, vol. 89, no. 3, pp. 267–282, Mar. 2009. https://doi.org/10.2522/ptj.20080130

[108] D. E. Vaillancourt, A. B. Slifkin, and K. M. Newell, "Regularity of force tremor in Parkinson's disease," *Clin. Neurophysiol.*, vol. 112, no. 9, pp. 1594–1603, Sep. 2001. https://doi.org/10.1016/S1388-2457(01)00593-4

[109] L. A. Sanchez-Perez, L. P. Sanchez-Fernandez, A. Shaout, J. M. Martinez-Hernandez, and M. J. Alvarez-Noriega, "Rest tremor quantification based on fuzzy inference systems and wearable sensors," *Int. J. Med. Inform.*, vol. 114, pp. 6–17, Jun. 2018. https://doi.org/10.1016/j.ijmedinf.2018.03.002

APPENDIX A

Short description of the features extracted from the signal. *N* is the total number of samples of the discrete time-series *x* of each window, *i* is the *i-th* discrete time instant, μ is the mean and σ the standard deviation of x.

Feature	Description	Formula
MAV	Mean absolute value	$MAV = \frac{1}{N}\sum_{i=1}^{N} \lvert x_i \rvert$
CV	Coefficient of variation	$CV = \frac{\sigma(x)}{\mu(x)}$
ZCR	Zero crossing rate	$ZCR = \frac{1}{2N}\sum_{i=1}^{N} \lvert sgn(x_{i+1}) - sgn(x_i) \rvert$ where $sgn(x_i) = \begin{cases} 1, & x_i \geq 0 \\ -1, & x_i < 0 \end{cases}$
SampEn	Sample entropy	$SampEn\ (m, r, N) = -log\frac{A}{B}$ where m is the length of the template (length of the window of the different vector comparisons) and r is tolerance which is usually selected as a factor of the standard deviation. For this application, we adopted m = 2 and r = 0.2 as in other studies [84][44]. B is the probability that two sequences are similar for *m* points, i.e., $d[X_m(i), X_m(j)] < r$. While A is the probability that two sequences are similar for m+1 points, i.e., $d[X_{m+1}(i), X_{m+1}(j)] < r$[77].
Hjorth parameters	Activity	$Activity = \sigma^2(x)$
	Mobility	$Mobility = \sqrt{\frac{Activity(\dot{x})}{Activity}}$ where $\dot{x}$ is the first discrete derivative of the x, i. e., $\dot{x} = \frac{x_i - x_{i-1}}{\Delta t}$ with temporal resolution $\Delta t = t_i - t_{i-1}$.
	Complexity	$Complexity = \sqrt{\frac{Mobility(\dot{x})}{Mobility}}$ where $\dot{x}$ is the first discrete derivative of the x, i. e., $\dot{x} = \frac{x_i - x_{i-1}}{\Delta t}$ with temporal resolution $\Delta t = t_i - t_{i-1}$.

Publications

[1] A. Rabelo *et al.*, “Identification and Characterization of Short-Term Motor Patterns in Rest Tremor of Individuals with Parkinson’s Disease,” *HealtHCare*, vol. 10, no. 12, p. 2536, Dec. 2022.

[2] S. Costa *et al.*, “Biomechanical Evaluation of an Exoskeleton for Rehabilitation of Individuals with Parkinson’s Disease,” *IRBM*, vol. 44, no. 1, p. 100741, Feb. 2023.

[3] Amanda Gomes Rabelo *et al*., “Evaluation of Hjorth parameters using synthetic signals,” XIIISBEB, 2021.

[4] Fabio Henrique Oliveira *et al.,* “ A non-contact system for the assessment of hand motor tasks in people with Parkinson’s disease, ” SN Applied Sciences, 2021.

[5] Depósito de patente (BR 10 2020 005222 5) - Dispositivo para monitoramento de indivíduos com a doença de parkinson; Amanda Rabelo, Adriano O. Andrade e Fabio Oliveira, 2020.

[6] Publicação de um capítulo de livro. Livro: Amanda Rabelo, R. M. A. Almeida e Adriano O. Andrade , “Avaliação Neurológica Funcional”. Capítulo: “Monitoramento de sintomas motores da doença de Parkinson utilizando dispositivos vestíveis,” (Appris Editora, 2020).

[7] Amanda Rabelo *et al.,* “ Low amplitude hand rest tremor assessment in Parkinson’s disease based on linear and nonlinear methods, ” CBEB, 2020.

[8] Apresentação do trabalho "Low amplitude hand rest tremor assessment in Parkinson’s disease based on linear and nonlinear methods" e participação no Congresso Brasileiro de Engenharia Biomédica, 2020.

[9] Adriano de Oliveira Andrade, Ana Paula Sousa Paixão, Ariana Moura Cabral, Amanda Gomes Rabelo, *et al*., “Task-Specific Tremor Quantification in a Clinical Setting for Parkinson’s Disease.,” Journal of Medical and Biological Engineering, 2020.

[10] Amanda Rabelo *et al.*, “Atividades realizadas utilizando tecnologias wearables durante a avaliação de indivíduos com a doença de Parkinson: Uma revisão sistemática, ” SEB, 2019.

[11] Samila Costa, Amanda Rabelo, *et al.*, "Análise do esforço muscular durante a execução dos movimentos de flexão e extensão de punho em pacientes com Doença de Parkinson - Um estudo piloto", SEB, 2019.

[12] Oliveira, Fabio Henrique M; Rabelo, Amanda, *et. al*, "On the use of Non-Contact Capacitive Sensors for the Assessment of Postural Hand Tremor of Individuals with Parkinson’s

Disease,"Annual International Conference of the IEEE Engineering in Medicine and Biology Society, 2019.

[13] L. Cláudio, V. Ferreira, A. G. Rabelo, M. F. Vieira, A. A. Pereira, and A. D. O. Andrade, "Gait variability and symmetry assessment with inertial sensors for quantitative discrimination of Trendelenburg sign in total hip arthroplasty patients : a pilot study based on convenience sampling ", Research on Biomedical Engineering, 2018.

[14] A. Rabelo, G. Jablonski, and L. Mai-, "A protocol for the quantification of simple reaction time : A case study," IFMBE Proc., vol. 2019.

[15] G. Jablonski *et al.*, "Quantification of the Finger Tapping Test Based on the Flex Sensor – A Single Case Study," IFMBE Proc., 2019.

[16] L. Luiz, A. Rabelo *et al.*, "On the Use Of Inertial Sensors For The Assessment Of Step And Stride Time Variability In Individuals with Parkinson ' s Disease : preliminary study," IFMBE Proc., 2019.

[17] S. Costa *et al.*, "Ergonomic Evaluation of an Active Wrist Orthosis for the Treatment of Muscular Rigidity in Individuals with Parkinson ' s Disease," IFMBE Proc., 2019.

[18] A. G. Rabelo *et al.*, "Uso da realidade virtual no tratamento de sintomas motores da doença de parkinson : uma revisão sistemática," in Simpósio Engenharia Biomédica, 2018.

[19] S. C. Costa *et al*., "Avaliação ergonômica da amplitude de movimento ao utilizar uma órtese ativa de punho - um estudo de caso, " Simpósio Engenharia Biomédica, 2018.

[20] Amanda Rabelo *et al.,* "Uma revisão dos métodos para avaliação da bradicinesia parkinsoniana utilizando sensores inerciais, " anais cobecseb, 2018.

[21] Cláudio L, Ferreira V, Rabelo AG *et.al*., "Gait variability and symmetry assessment with inertial sensors for quantitative discrimination of Trendelenburg sign in total hip arthroplasty patients: a pilot study based on convenience sampling, " Research on Biomedical Engineering, 2018.

[22] Rabelo, Amanda Gomes *et. al,* "Objective Assessment of Bradykinesia Estimated from the Wrist Extension in Older Adults and Patients with Parkinson's Disease, " Annals of biomedical engineering, v. 45, p. 2614-2625, 2017.

[23] Andrade, Adriano O. ; Ferreira, Luiz Cláudio Vieira ; Rabelo, Amanda g. et al., "Pelvic movement variability of healthy and unilateral hip joint involvement individuals, "Biomedical Signal Processing and Control, v. 32, p. 10-19, 2017.